ORIGINAL ARTICLE

MOLECULAR ECOLOGY WILEY

Multiple types of genomic variation contribute to adaptive traits in the mustelid subfamily Guloninae

Lorena Derežanin[1] | Asta Blažytė[2] | Pavel Dobrynin[3] | David A. Duchêne[4] | José Horacio Grau[5] | Sungwon Jeon[2] | Sergei Kliver[6] | Klaus-Peter Koepfli[3,7,8] | Dorina Meneghini[1] | Michaela Preick[9] | Andrey Tomarovsky[3,6,10] | Azamat Totikov[3,6,10] | Jörns Fickel[1,9] | Daniel W. Förster[1]

[1]Leibniz Institute for Zoo and Wildlife Research (IZW), Berlin, Germany

[2]Department of Biomedical Engineering, College of Information and Biotechnology, Ulsan National Institute of Science and Technology (UNIST), Ulsan, Korea

[3]Computer Technologies Laboratory, ITMO University, Saint Petersburg, Russia

[4]Center for Evolutionary Hologenomics, The GLOBE Institute, Faculty of Health and Medical Sciences, University of Copenhagen, Copenhagen, Denmark

[5]Amedes Genetics, amedes Medizinische Dienstleistungen GmbH, Berlin, Germany

[6]Institute of Molecular and Cellular Biology, SB RAS, Novosibirsk, Russia

[7]Smithsonian-Mason School of Conservation, Front Royal, Virginia, USA

[8]Center for Species Survival, Smithsonian Conservation Biology Institute, National Zoological Park, Front Royal, Virginia, USA

[9]Institute for Biochemistry and Biology, Faculty of Mathematics and Natural Sciences, University of Potsdam, Potsdam OT Golm, Germany

[10]Novosibirsk State University, Novosibirsk, Russia

Correspondence
Lorena Derežanin, Leibniz Institute for Zoo and Wildlife Research (IZW), Alfred Kowalke Straße 17, 10315 Berlin, Germany.
Email: lorenaderezanin@gmail.com

Present address
Sungwon Jeon, Clinomics Inc., Ulsan, Korea

Funding information
Russian Foundation for Basic Research, Grant/Award Number: 0-04-00808; Carlsbergfondet, Grant/Award Number: CF18-0223

Handling Editor: Andrew DeWoody

Abstract

Species of the mustelid subfamily Guloninae inhabit diverse habitats on multiple continents, and occupy a variety of ecological niches. They differ in feeding ecologies, reproductive strategies and morphological adaptations. To identify candidate loci associated with adaptations to their respective environments, we generated a *de novo* assembly of the tayra (*Eira barbara*), the earliest diverging species in the subfamily, and compared this with the genomes available for the wolverine (*Gulo gulo*) and the sable (*Martes zibellina*). Our comparative genomic analyses included searching for signs of positive selection, examining changes in gene family sizes and searching for species-specific structural variants. Among candidate loci associated with phenotypic traits, we observed many related to diet, body condition and reproduction. For example, for the tayra, which has an atypical gulonine reproductive strategy of aseasonal breeding, we observed species-specific changes in many pregnancy-related genes. For the wolverine, a circumpolar hypercarnivore that must cope with seasonal food scarcity, we observed many changes in genes associated with diet and body condition. All types of genomic variation examined (single nucleotide polymorphisms, gene family expansions, structural variants) contributed substantially to the identification of candidate

loci. This argues strongly for consideration of variation other than single nucleotide polymorphisms in comparative genomics studies aiming to identify loci of adaptive significance.

1 | INTRODUCTION

The Mustelidae are the most ecologically and taxonomically diverse family within the mammalian order Carnivora, representing a remarkable example of adaptive radiation among mammals that is rich with recent speciation events (Koepfli et al., 2008; Liu et al., 2020). Closely related mustelid species often inhabit vastly different ecosystems, where they experience diverse environmental challenges and are thus exposed to different evolutionary pressures. This is particularly pronounced in the mustelid subfamily Guloninae, within which species occupy a variety of ecological niches, ranging from scansorial (adapted to climbing) omnivores in the neotropics to terrestrial hypercarnivores in circumpolar regions. Members of the Guloninae display a range of behavioural and physiological

adaptations associated with environment-specific resource availability, and consequently differ markedly in feeding ecology, reproductive strategy and morphology (Heldstab et al., 2018; Zhou et al., 2011). Here, we focus on tayra, wolverine and sable (Figure 1), for which genomic resources are now available.

The tayra (*Eira barbara*) is a predominantly diurnal, solitary species that inhabits tropical and subtropical forests of Central and South America, ranging from Mexico to northern Argentina (Wilson & Mittermeier, 2009). It is a scansorial, opportunistic omnivore, feeding on fruits, small mammals, birds, reptiles, invertebrates and carrion. Caching of unripe fruit for later consumption has been observed (Soley & Alvarado-Díaz, 2011). Unlike other gulonine species, which are characterized by seasonal breeding and embryonic diapause, the tayra is an aseasonal polyoestrous
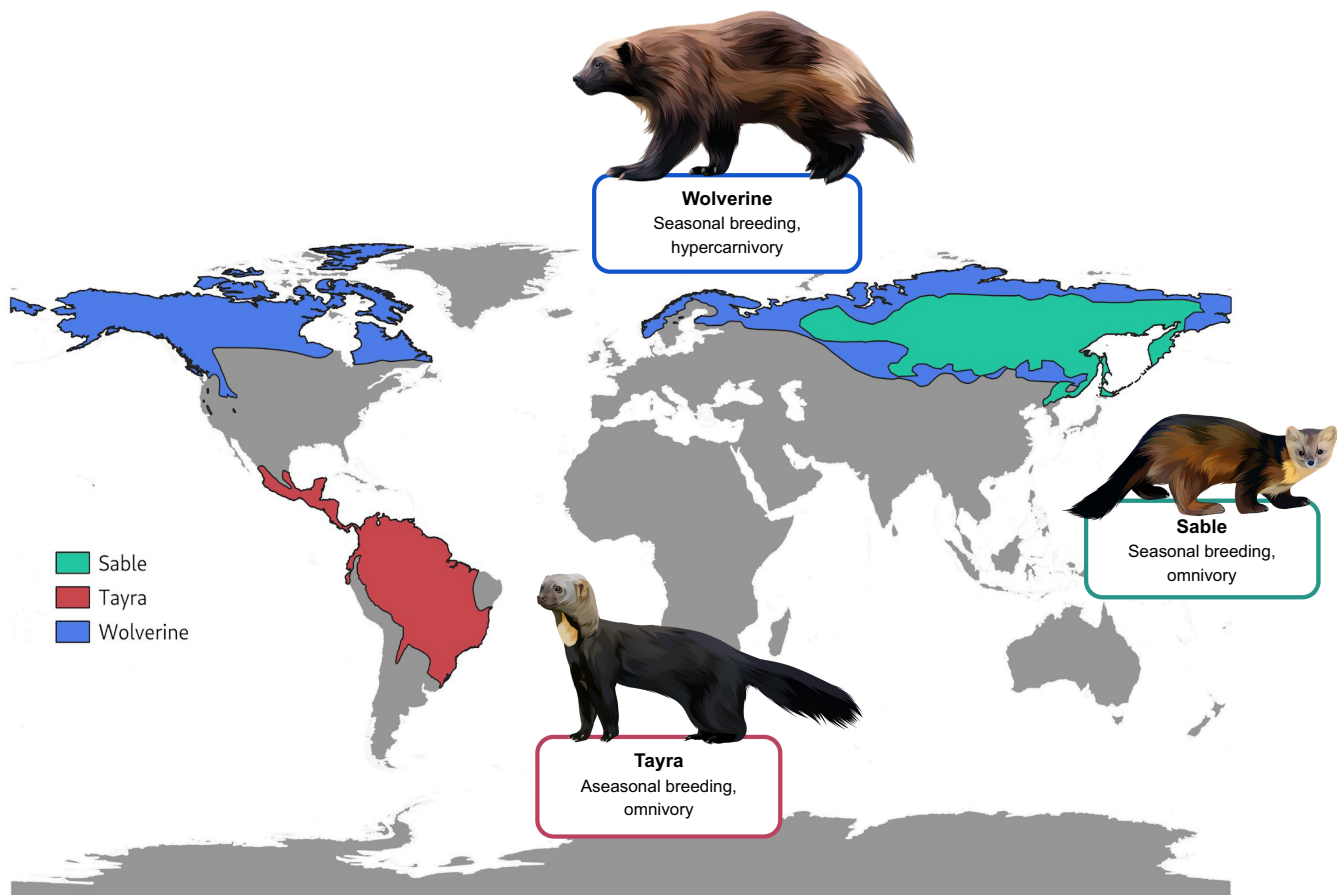
FIGURE 1 Distribution and species-specific traits of the tayra (*Eira barbara*), wolverine (*Gulo gulo*) and sable (*Martes zibellina*). Vector graphics of species are created based on royalty-free images (Source: Shutterstock)

breeder and does not exhibit delayed implantation (Proulx & Aubry, 2017), which may be due to the less prominent seasonality and fluctuation in food availability in neotropical habitats (Heldstab et al., 2018).

The largest terrestrial mustelid, the wolverine (*Gulo gulo*), is a circumpolar species, inhabiting alpine and boreal zones across North America and Eurasia (Ekblom et al., 2018). The wolverine is an opportunistic predator and facultative scavenger, either feeding on carrion or actively hunting medium- to large-sized mammals, such as roe deer, wild sheep and occasionally moose (Pasitschniak-Arts & Larivière, 1995). Morphological and behavioural adaptations such as dense fur, plantigrade locomotion facilitating movement through deep snow, and food caching enable wolverines to survive in cold habitats with limited food resources (Copeland & Kucera, 1997). In addition, wolverines occupy large home ranges, and display territoriality, seasonal breeding and delayed implantation, traits indicating an adaptive response necessary for survival in scarce resource environments (Inman et al., 2012).

The sable (*Martes zibellina*) is distributed in the taiga and deciduous forests of north central and northeastern Eurasia. The sable is solitary and omnivorous, relying on hearing and olfaction to locate prey, even under snow cover during winter months (Liu et al., 2020; Monakhov, 2011). Unlike wolverines, seasonal changes do not cause dramatic fluctuations in resource availability for sables as they are able to exploit a wider variety of food sources, and are adapted to tolerate short-term food scarcity (Mustonen et al., 2006). Their diet consists of small mammals, birds, nuts and berries, and in some instances food caching during the winter period has been reported (Monakhov, 2011). Similar to wolverines and many other species of mustelids, sables have a well-defined reproductive season and exhibit delayed blastocyst implantation (Proulx & Aubry, 2017).

To date, only a few studies have investigated adaptive variation in mustelids using comparative genomics (Abduriyim et al., 2019; Beichman et al., 2019; Liu et al., 2020; Miranda et al., 2021). Here, we generated a highly contiguous genome assembly of the tayra, an early diverging gulonine (Koepfli et al., 2008; Law et al., 2018), and compared it to previously published genomes of the wolverine and sable to identify the genetic basis underlying the adaptations to the diverse environments inhabited by these species.

In addition to identifying genes under positive selection, we investigated gene family evolution and structural variants (SVs), as these types of variants represent a significant source of intra- and interspecific genomic differentiation, affecting more nucleotides than single-nucleotide polymorphisms (SNPs) (Catanach et al., 2019). Gene copy number variation and large SVs can be associated with an adaptive response to new ecological circumstances (Rinker et al., 2019), and are thus an important source of genomic novelty to consider when studying adaptive divergence among species (Hecker et al., 2019). We focused on candidate loci linked to species-specific traits associated with response to environmental challenges, such as resource availability in the respective habitats of our study species.

2 | MATERIALS AND METHODS

2.1 | Sequencing, genome assembly and alignment

Whole blood from a captive (second-generation) male tayra was collected by the veterinary staff of the "Wildkatzenzentrum Felidae," Barnim (Germany), during a routine medical checkup. High-molecular-weight (HMW) genomic DNA extraction was performed using the Qiagen MagAttract HMW DNA Kit, following the manufacturer's protocol. We used 1 ng of DNA and the Chromium Genome Reagents Kits Version 2 and the 10× Genomics Chromium Controller instrument with a microfluidic chip for library preparation. Sequencing was carried out on an Illumina NovaSeq 6000 with 300 cycles on an S1 lane.

We generated a *de novo* genome assembly using the 10x Genomics Supernova assembler version 2.1.1 (Weisenfeld et al., 2017) with default parameters (assembly metrics given in Table 1; Table S1). The assemblies of tayra (this study, JAHRIG000000000), wolverine (Ekblom et al., 2018; GCA_900006375.2), sable (Liu et al., 2020; GCA_012583365.1) and domestic ferret (MusPutFur1.0_HiC; Dudchenko et al., 2017, 2018; Peng et al., 2014) were assessed for gene completeness with BUSCO version 4.1.2 using the mammalian lineage data set mammalia_odb10 (Simão et al., 2015). To accurately identify repeat families, we used REPEATMODELER version 2 (Flynn et al., 2020) with the "-LTRstruct" option, followed by REPEATMASKER version 4.1.2 (Smit, 2004) to identify and mask the modelled repeats in the tayra genome assembly.

2.2 | Demographic reconstruction

Trimmed reads of all three gulonine were mapped to their respective genomes in local mode with BOWTIE2 version 2.3.5.1 (Langmead & Salzberg, 2012), and analysis of demographic history was performed with PSMC version 0.6.5 (Li & Durbin, 2011) using the following parameters (repeated 100 times for bootstrapping): *psmc -N25 -t15 -r5 -b -p '4+25*2+4+6' -o round-${ARRAY_TASK_ID}.psmc ${name}.split.psmcfa*. Results for each genome were plotted with psmc_plot.pl, and the mutation rate was set to 1e-08 substitutions per site per generation (Cahill et al., 2016; Dobrynin et al., 2015). Generation times were set to 7.4 years for tayra, 5.7 years for sable (Pacifici et al., 2013) and 6 years for wolverine (Ekblom et al., 2018).

2.3 | Reference-based scaffolding

Using the domestic ferret genome as a reference, we generated pseudochromosome assemblies for tayra, wolverine and sable, to visualize heterozygosity along chromosomes. Scaffolding was performed using RAGOO version 1.1 (Alonge et al., 2019). The X chromosome in the domestic ferret assembly was identified via whole genome alignment to the domestic cat (*Felis catus*) Felis_catus_9.0 assembly (Buckley et al., 2020) and ZooFISH data available from

TABLE 1 Comparison of genome assembly metrics among four mustelid species

	Tayra (*Eira barbara*)	Domestic ferret (*Mustela putorius furo*)	Sable (*Martes zibellina*)	Wolverine (*Gulo gulo*)
Assembly accession/ reference	JAHRIG000000000 (this study)	MusPutFur1.0_HiC (Dudchenko et al., 2017, 2018; Peng et al., 2014) GCF_000215625.1 (Dudchenko et al., 2017, 2018; Peng et al., 2014)	GCA_012583365.1 (Liu et al., 2020)	GCA_900006375.2 (Ekblom et al., 2018)
Sequencing/assembly approach	Illumina + 10× Genomics/ Supernova	Illumina/ALLPATHS-LG + Hi-C scaffolding	Illumina/SOAPDENOVO2	Illumina/SOAPDENOVO
Raw coverage (×)	75.6	162	114.5	76
Contig N50 (kb)	289.9	44.7	41.7	3.6
Scaffold N50 (Mb)	42.0	145.3	5.2	0.2
Number of scaffolds	14,579	7428	15,814	47,417
Total genome length (Gb)	2.44	2.40	2.42	2.42

the *Atlas of Mammalian Chromosomes* (Cavagna et al., 2000; O'Brien et al., 2020). Whole genome alignment was performed using LAST version 971 (Frith & Kawaguchi, 2015).

Variant calling followed by quality filtration was performed using the BCFTOOLS pipeline version 1.10 (Poplin et al., 2018). Low-quality variants were removed (BCFTOOLS filter, "QUAL < 20.0 || (FORMAT/SP > 60.0 || FORMAT/DP < 5.0 || FORMAT/GQ < 20.0)"). In each sample, positions with coverage lower or higher than 50%–250% of the whole genome median value were removed. Of the remaining positions only those common to all samples were retained. Finally, SNPs with uncalled genotypes in any sample and variants with the same genotypes for all samples were removed. For visualization, heterozygous SNPs were counted in nonoverlapping sliding windows of 1 Mbp (counts scaled to SNPs per kbp). Indels were not included due to the low quality of calls from short reads. SNP density plots were created using the MACE package (https://github.com/mahajrod/MACE).

2.4 | Phylogenomic data preparation, analysis and dating

We performed sequence alignments and filtering of excessively divergent segments in each of 6020 coding genomic regions of single-copy orthologues shared across eight species of carnivores, using the software MACSE version 2 (Ranwez et al., 2011). Our taxon set included domestic cat (*Felis catus*), domestic dog (*Canis familiaris*), northern elephant seal (*Mirounga angustirostris*) and walrus (*Odobenus rosmarus*), in addition to four mustelid species. To extract the most reliable signal from these coding data, we excluded whole alignments that were excessively divergent, contained excessive missing data or violated basic substitution model assumptions (further details in the Supporting Information). This led to a phylogenomic data set with 2457 gene regions comprising over 3.2 million nucleotide sites. Gene trees were estimated from

gene regions by first selecting the best substitution model from the GTR+F+Γ+I+R family (Kalyaanamoorthy et al., 2017), and calculating approximate likelihood-ratio test (aLRT) branch supports (Anisimova & Gascuel, 2006), as implemented in IQ-TREE version 2 (Minh et al., 2020a,b).

Species tree estimates were performed using (i) concatenated sequence alignments for maximum-likelihood inference using IQ-TREE version 2, and (ii) gene trees for inference under the multispecies coalescent using the summary coalescent method in ASTRAL-III (Zhang et al., 2018). The maximum-likelihood estimate of the species tree was accompanied by aLRT branch supports, while summary coalescent inference was accompanied by local posterior probabilities (Sayyari & Mirarab, 2016). The decisiveness of the data regarding the phylogenetic signals was examined using gene- and site-concordance factors, calculated in IQ-TREE version 2 (Minh, Schmidt, et al., 2020).

Bayesian molecular dating analysis was performed using MCMCtree in PAML version 4.8 (Yang, 2007). To minimize the violation of the time-tree prior (Angelis & Dos Reis, 2015) and the negative impact of gene tree discordance on rate estimates (Mendes & Hahn, 2016), we only included genomic regions with gene trees concordant with the species tree, and assumed the reconstructed species tree from ASTRAL-III (see Supporting Information for further details). This led to a data set for molecular dating that included 992 single-copy orthologous gene regions, comprising 0.53 million sites. The data were partitioned by codon positions, each modelled under individual GTR+Γ substitution models. We used an uncorrelated gamma prior on rates across lineages and a birth–death prior for divergence times. Fossil calibrations are listed in the Supporting Information. The posterior distribution was sampled every 1×10^3 Markov chain Monte Carlo (MCMC) steps over 1×10^7 steps, after a burn-in phase of 1×10^6 steps. We verified convergence to the stationary distribution by comparing the results from two independent runs, and confirming that the effective sample sizes for all parameters were above 1,000 using the R package coda (Plummer et al., 2006).

2.5 | Positive selection on single-copy orthologues

To investigate genes under positive selection, the coding sequences (CDS) corresponding to 1:1 orthologues were aligned for the eight aforementioned carnivoran species. Multiple sequence alignments (MSAs) were constructed with PRANK version 120716 (Löytynoja, 2014), and 17 MSAs were removed due to short alignment length. The CODEML module in the PAML version 4.5 package was used to estimate the ratio of nonsynonymous to synonymous substitutions, also called d_N/d_S or ω (Yang, 2007). We applied the one-ratio model to estimate the general selective pressure acting among all species, allowing only a single d_N/d_S ratio for all branches. A free-ratio model was also used to estimate the d_N/d_S ratio of each branch. Furthermore, the CODEML branch-site test for positive selection was performed on 6003 orthologue alignments for three separate foreground branches: *Eira barbara*, *Gulo gulo* and *Martes zibellina* (Zhang et al., 2005). Statistical significance was assessed using likelihood ratio tests (LRTs) with a conservative 10% false discovery rate (FDR) criterion (Nielsen et al., 2005). Orthologues with a free-ratio >2 in the branch model were considered for further analysis of signatures of positive selection.

To account for differences in genome assembly quality, we evaluated the alignments of selected orthologues based on the transitive consistency score (TCS), an extension to the T-Coffee scoring scheme used to determine the most accurate positions in MSAs (Chang et al., 2014). Additionally, alignments were visually inspected for potential low-scoring MSA portions.

2.6 | Gene family evolution

To investigate changes in gene family sizes, we constructed a matrix containing 7838 orthologues present as either complete "single-copy," complete "duplicated" or "missing," identified using the BUSCO genome assembly completeness assessment of all eight carnivoran genomes. Orthologues were retained if they were detected in at least four species (including *Felis catus* as an outgroup) to obtain meaningful likelihood scores for the global birth and death (λ) parameter.

We applied a probabilistic global birth and death rate model of CAFE version 4.2.1. (Han et al., 2013) to analyse gene gains ("birth") and losses ("death") accounting for phylogenetic history. First, we estimated the error distribution in our data set, as genome assembly and annotation errors can result in biased estimates of the average rate of change (λ), potentially leading to an overestimation of λ. Following the error distribution modelling, we ran the CAFE analysis guided by the ultrametric tree estimated earlier, calculating a single λ parameter for the whole species tree. The CAFE results were summarized (Table S4A) with the python script *cafetutorial_report_analysis.py* (https://github.com/hahnlab/CAFE).

We examined differences between duplicates arising through gene family expansion, to determine how these paralogues differed and if a signal of selection could be detected. Pairwise codon-aware sequence alignment of paralogues was performed with DIALIGN-TX

version 1.0.2 (Subramanian et al., 2008). Ratios of nonsynonymous to synonymous substitution rates were estimated using KAKS_CALCULATOR version 2.0 (Zhang et al., 2006; details are given in the Supporting Information). Paralogues with identical nucleotide sequences were considered to be recent duplications ("NAs" in Table S5B).

2.7 | Structural variation

To avoid reference genome bias, preprocessed reads from the three Guloninae were aligned to the domestic ferret (*Mustela putorius furo*) genome with BOWTIE2 version 2.3.5.1 (Langmead & Salzberg, 2012) (details given in Supporting Information). Duplicated reads were removed with PICARD TOOLKIT version 2.23 (MarkDuplicates, Broad Institute, 2019). Trimmed tayra reads were downsampled to ~38× with SEQTK version 1.3 (https://github.com/lh3/seqtk) prior to mapping to maintain uniformity among libraries and to avoid bias in variant calling.

We applied an ensemble approach for SV calling, encompassing three SV callers: MANTA version 1.6.0 (Chen et al., 2016), WHAMG version 1.7.0 (Kronenberg et al., 2015) and LUMPY version 0.2.13 (Layer et al., 2014). SV calls originating from reads mapping in low-complexity regions and with poor mapping quality were removed from all three call sets. We retained MANTA calls with paired-read (PR) and split-read (SR) support of PR ≥ 3 and SR ≥ 3, respectively. To reduce the number of false positive calls, the WHAMG call set was filtered for potential translocation events, as WHAMG flags but does not specifically call translocations. We further removed calls with a low number of reads supporting the variant (PR, SR) from the WHAMG (A < 10) and the LUMPY call set (SU <10). All SV call sets were filtered based on genotype quality (GQ ≥ 30). WHAMG and LUMPY SV call sets were genotyped with SVTYPER version 0.7.1 (Chiang et al., 2015) prior to filtering. Only scaffolds assigned to chromosomes were included in further analyses. SURVIVOR version 1.0.7 (Jeffares et al., 2017) was used to merge and compare SV call sets within and among samples. The union set of SV calls among the three gulonine species containing species-specific and shared variants was annotated, using LIFTOFF version 1.5.1 (Shumate & Salzberg, 2020), for preparation of reference genome annotation, and Ensembl Variant Effect Predictor version 101.0 (McLaren et al., 2016) for identifying variants affecting protein-coding genes. Gene ontology analysis was performed with SHINY GO (Ge et al., 2020) with an FDR < 0.05 for each SV type (excluding inversions) overlapping multiple protein-coding genes (more than five genes).

2.8 | Candidate loci

The functional and biological roles of positively selected genes, loci affected by changes in gene family size, and structural variants, were explored using literature sources and online databases, including OrthoDB version 10 (Kriventseva et al., 2019), Uniprot (The UniProt Consortium, 2017) and NCBI Entrez Gene (Maglott et al., 2011).

Gene descriptions, GO biological processes, functions and relevant citations are provided in the supporting tables (see below). Gene Ontology enrichment analysis was performed with SHINY GO version 0.65 (Ge et al., 2020), for gene sets obtained from previously mentioned analyses (positive selection on single genes, PSG; gene family evolution, GF; and SV) for the three gulonine species. Gene sets were inspected for significant enrichment of biological processes with the following parameters: best matching species, top 10 pathways, and FDR p-value cutoff.05. SHINY GO version 0.65 is based on a database derived from Ensembl Release 103.

3 | RESULTS

3.1 | Genome assembly

We generated a highly contiguous reference genome assembly for the tayra (*Eira barbara*). Extracted genomic DNA had an average molecular size of 50.75 kb and was sequenced to ~76-fold coverage (Table S1). The final assembly showed a total length of ~2.44 Gb (excluding scaffolds shorter than 5 kb), with a contig N50 of 290 kb, scaffold N50 of 42.1 Mb, and identity in 95% of all positions in an alignment with the domestic ferret genome (Figure S1). The tayra assembly has higher contiguity than the Illumina-only-based assemblies of both wolverine and sable, but it is more fragmented than the chromosome-length domestic ferret (*Mustela putorius furo*) assembly (Table 1; Figure S2A) that we used as a reference genome for some analyses. The haploid tayra genome of ~2.4 Gb is contained in 162 scaffolds (>100 kb) with 40 scaffolds having a length above 50 Mb (Figure S2A).

The tayra assembly has high gene completeness as assessed with BUSCO version 4.1.2 using 9226 conserved mammalian orthologues in total, 8540 (92.5%) complete benchmarking Universal Single-Copy Orthologs (BUSCOs) were identified, encompassing 8492 (92.0%) of complete and single-copy, and 48 (0.5%) complete and duplicated orthologues. Additionally, 104 (1.1%) orthologues were fragmented and 582 (6.4%) were missing. As measured by this metric, the tayra genome has higher gene completeness than the published genomes of wolverine, sable or domestic ferret (Figure S2B).

3.2 | Repetitive elements

The repeat landscape of the tayra assembly contains ~0.85 Gb of repetitive elements (Table S2). L1 type LINE elements are the most abundant, constituting 23% of the tayra genome. L1 elements also show signs of recent proliferation in comparison to DNA transposons and LTR retroelements (Figure S3). Endogenous retroviruses constitute 3.8% of the tayra genome and can be classified as Gammaretroviruses and Betaretroviruses.

The overall repeat landscape of the tayra genome assembly is comparable to other carnivore genomes (Liu et al., 2020; Peng et al., 2018). It is similar to that of the sable genome, differing mostly in the number of L1 LINE elements, which have been recently proliferating and accumulating within the tayra genome more than in other Guloninae genomes. The diversity of endogenous retroviruses is similar to that of other mustelids. Although endogenous delta-retroviruses have been described from a broad range of mammal genomes, including several smaller carnivores such as mongoose (family Herpestidae) and the fossa (*Cryptoprocta ferox*) (Hron et al., 2019), no delta-retroviruses were found in the genome of tayra.

3.3 | Demographic reconstruction

Reconstruction of historical demography for tayra, wolverine and sable, using the Pairwise Sequentially Markovian Coalescent model (PSMC; Li & Durbin, 2011) revealed different trends in effective population sizes (N_e) (Figure S4). While the trajectories for all three species involve multiple declines and rebounds in N_e, the timing, duration and magnitude of these differ. In tayras, there are three extensive declines beginning around 4.5 million years ago (Ma) (>35% reduction in N_e), 500 thousand years ago (ka) (>30%) and 80 ka (>80%), resulting in a recent N_e of ~14,000 individuals. In wolverines, a sharp decline 1 Ma (>45%) is followed by a plateau in N_e and subsequent decline beginning ~400 ka (>30%), followed by a moderate rebound and final decline beginning 40 ka (>80%), resulting in a recent N_e of ~2,500 individuals. In sable, N_e gradually declines until ~500 ka (>40%), followed by a moderate rebound and sharp decline around 200 ka (>40%). This is followed by an extensive rebound beginning 100 ka and subsequent sharp declines 50 ka (>30%) and 15 ka (>50%), resulting in a recent N_e of ~23,000 individuals. Thus, all three species exhibit complex historical trends in N_e, with little overlap in timing or magnitude.

Consistent with Ekblom et al. (2018), we observe low recent N_e in wolverines. However, our reconstructed trajectory of historical N_e for the wolverine differs from that of Ekblom et al. (2018), probably owing to different PSMC parameters. That notwithstanding, the timing and relative magnitude of the final decline is in broad agreement in the two studies.

3.4 | Nucleotide diversity

The tayra, sable and wolverine assemblies were generated using different approaches and differ significantly in contiguity (Table 1). To compare nucleotide diversity among the Guloninae, we generated pseudochromosome assemblies for each species using the chromosome-length assembly of the domestic ferret as a reference. The domestic ferret has more chromosomes than the other species ($2n = 40$ vs. $2n = 38$), and the same number (20) of pseudochromosomes (Lewin et al., 2019) were obtained after scaffolding in each case. For each assembly, we identified the X chromosome (labelled as *ps_chrX*) and arranged pseudoautosomes (labelled as *ps_aut1* – *ps_aut19*) according to the length of the original scaffolds in the domestic ferret reference. This allowed us to verify the sex of the

animals using a coverage-based approach (Figure S5), which confirmed morphological sexing for the tayra (male) and wolverine (female) individuals. While the sable individual is referred to as a male (Liu et al., 2020), our analysis suggests it is a female (further details given in Supporting Information).

We counted heterozygous SNPs in 1-Mbp stacking windows for all three species and scaled it to SNPs per kbp (Figure 2). Median values for tayra, sable and wolverine were 1.89, 1.44 and 0.28 SNPs per kbp, respectively, the last being in agreement with previous findings (Ekblom et al., 2018). All scaffolds of ≥1 Mbp in pseudochromosome assemblies were taken into account. Exclusion of ps_chrX resulted in slight increases of medians to 1.93, 1.47 and 0.29, respectively (Table S3, Figure S6). Regardless of whether ps_chrX was included or excluded, the genome-wide diversities among the three species were significantly different ($p \ll 0.001$, Mann–Whitney test).

3.5 | Phylogenomics and molecular dating

We reconstructed the phylogenetic relationships of the following carnivoran species: domestic cat, domestic dog, walrus, northern elephant seal, domestic ferret, wolverine, sable and tayra. Phylogenomic analyses using concatenation and summary coalescent methods led to an identical resolution of the relationships among mustelid taxa. Within Guloninae, the wolverine and sable were placed as sisters, to the exclusion of the tayra (Figure 3). Branch supports were maximal across all branches using both aLRT and local posterior probabilities. Similarly, concordance factors for genes and sites (gCF, sCF) were high across branches and consistently more than twice as high as the values of the discordance factors (gDF, sDF). The lowest concordance factors were those in support of the resolution of *Gulo* and *Martes* as sisters (gCF = 64.52, sCF = 54.38). However, the discordance factors were less than half these values (gDF < 14, sDF < 24), suggesting substantial decisiveness across genes and sites for this resolution.

Divergence time estimates across mustelids were largely in agreement with previous findings (Koepfli et al., 2008; Law et al., 2018; Li et al., 2014; Sato et al., 2012), placing the split between *Mustela* and Guloninae at 11.2 Ma (highest posterior density interval (HPDI) between 13.1 and 9.5 Ma), and the split between *Eira* and the *Gulo–Martes* group at 7.5 Ma (HPDI between 9 and 6.1 Ma). The split between *Gulo* and *Martes* was dated at 5.9 Ma (HPDI between 7.4 and 4.7 Ma).

3.6 | Positive selection on single-copy orthologues

In the three Guloninae species, we found sites under positive selection ($5 > d_N/d_S > 1$; Barnett et al., 2020) in 55 single-copy orthologues that were highly significant (free-ratio > 2). Of these 55 positively selected genes (PSGs), 15 were observed in tayra, 22 in wolverine and 18 in sable (Figure 4a,b). Gene names, descriptions and functions are given in Table S4.

Among the 15 PSGs we detected in tayra, five are associated with reproduction (*NSMCE1*, *ETV2*, *SPATA25*, *MUC15* and *PIH1D2*) with functions involving spermatogenesis, placenta and embryo development, and blood vessel morphogenesis. Among the remaining 10 PSGs, *HSPB6* is involved in vasodilation and muscle contraction, *DERA* is associated with environmental stressors, including exposure to toxins, and uricase (*UOX*) is a liver enzyme involved in purine catabolism and regulation of fructose metabolism. Three PSGs (*IP6K3*, *MAGIX* and *FAM149B1*) are found to be associated with the nervous system, synapse formation and structural plasticity, as well as motor skills and coordination. Three further PSGs (*DUSP19*, *TNLG2B* and *LRRC46*) are related to the immune system and *HEMK1* regulates methylation processes. Gene enrichment analysis revealed an overrepresentation of genes in gene ontology (GO) categories associated with reproduction (Table S4A; GO:0046483, "Heterocycle metabolic process," $p = .022$) and metabolism/energy conversion (Table S4A, multiple pathways, $p < .03$).

We detected 22 PSGs in wolverine, including six genes associated with energy production and conversion. Among them, *ATP6V0B*, *KMO* and *SLC16A4* are primarily involved in insulin level regulation, and the metabolism of carbohydrates and fatty acids. Three PSGs (*OIP5*, *ZADH2* and *MTPAP*) are specifically associated with adipose tissue formation and intramuscular fat deposition. Additionally, we found three PSGs (*NBR1*, *TMEM38B*, *PPP1R18*) involved in selective autophagy as a response to nutrient deprivation along with bone mass and density regulation, and resorption. We also detected PSGs (*DAB1*, *OPA1* and *CTNS*) linked to cognition, brain development and vision. Several PSGs (*BNIPL*, *IL18BP*, *CRNN*) were associated with the immune system; three others (*ANAPC7*, *RNF212B*, *IZUMO3*) are involved in reproduction processes and *USB1* and *CLCN4* have a role in basal cell cycle processes. For the remaining two, *CEP95* and *FAM185A*, it was not possible to associate a specific phenotypic trait. No overrepresentation of GO categories was detected.

Among the 18 PSGs detected in sable, three (*PRRT2*, *ATL2*, *SELENOI*) are associated with locomotion and coordination, and *USP53* is associated with sensory perception and the nervous system. Two PSGs, *VEGFC* and *RASA1*, are associated with blood vessel formation, three (*TTC4*, *ZBP1*, *CD247*) with the immune system and three (*IQUB*, *UBQLNL*, *MEIKIN*) with reproduction. Several PSGs (*EEF2KMT*, *DEUP1*, *ECD*, *IQCK*) are associated with cell cycle processes, while *ZC2HC1C* and *CCDC17* could not be associated with a particular biological process. Gene enrichment analysis revealed an overrepresentation of GO categories associated with ear morphogenesis (Table S4A, multiple pathways, $p < .05$).

FIGURE 2 Heterozygosity density among pseudochromosomes for (a) tayra, (b) sable and (c) wolverine. Heterozygous SNPs were counted in stacking windows of 1 Mbp and scaled to SNPs per kbp. Tayra is a male individual and thus heterozygous SNP density is underestimated (due to only one X chromosome), while sable and wolverine are females and therefore likely to be representative of true SNP density
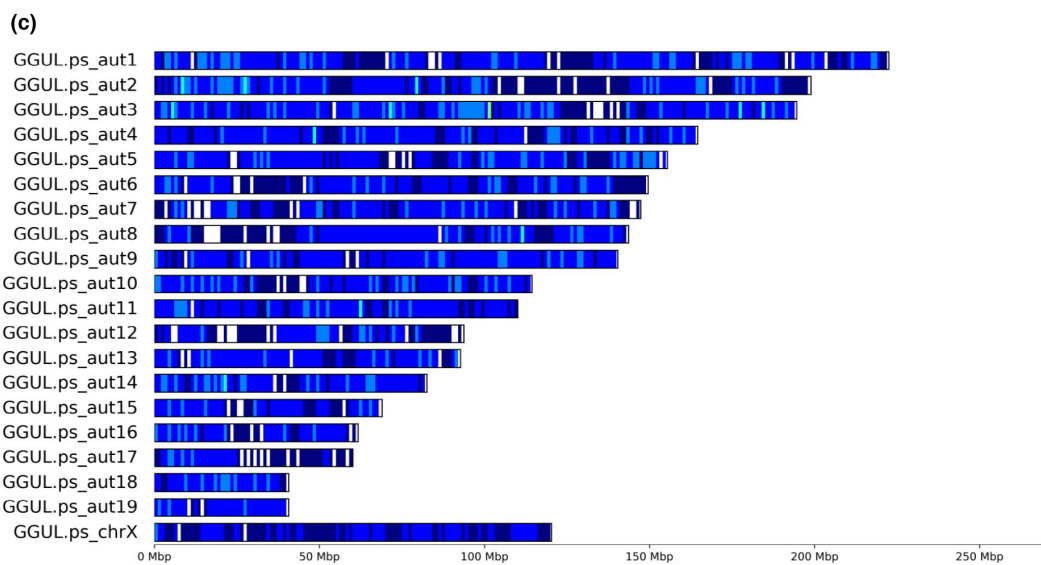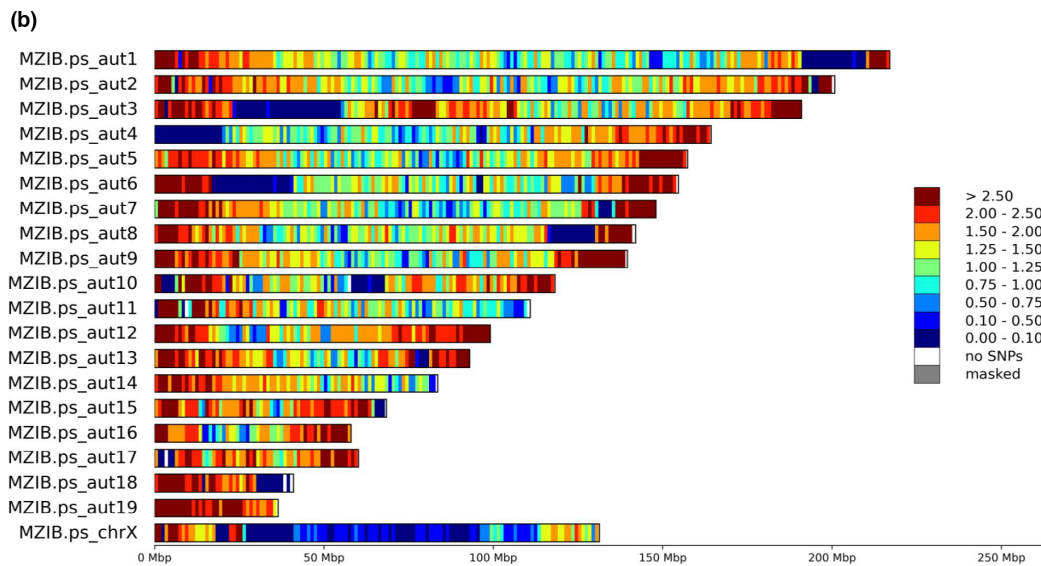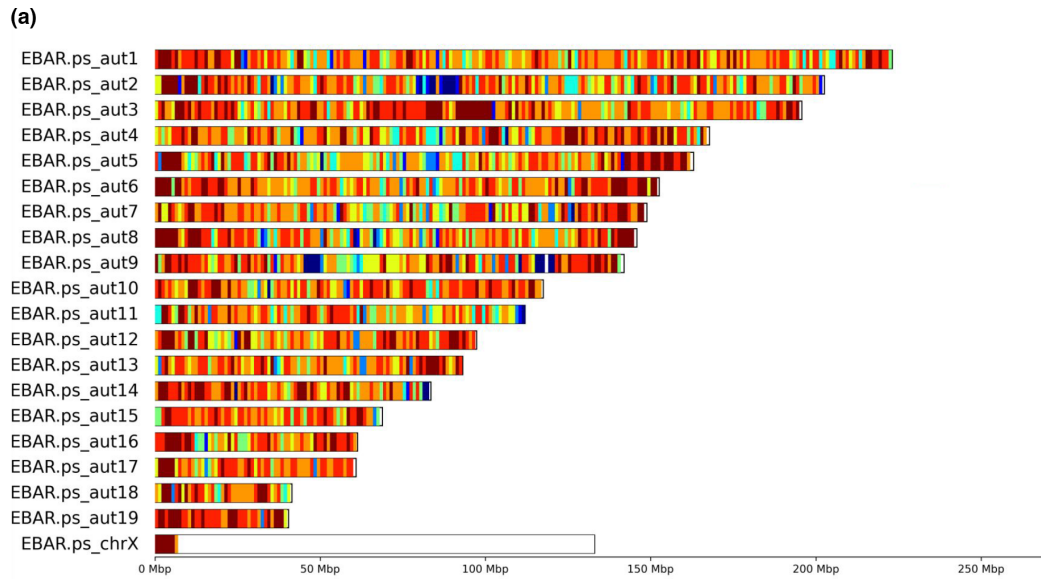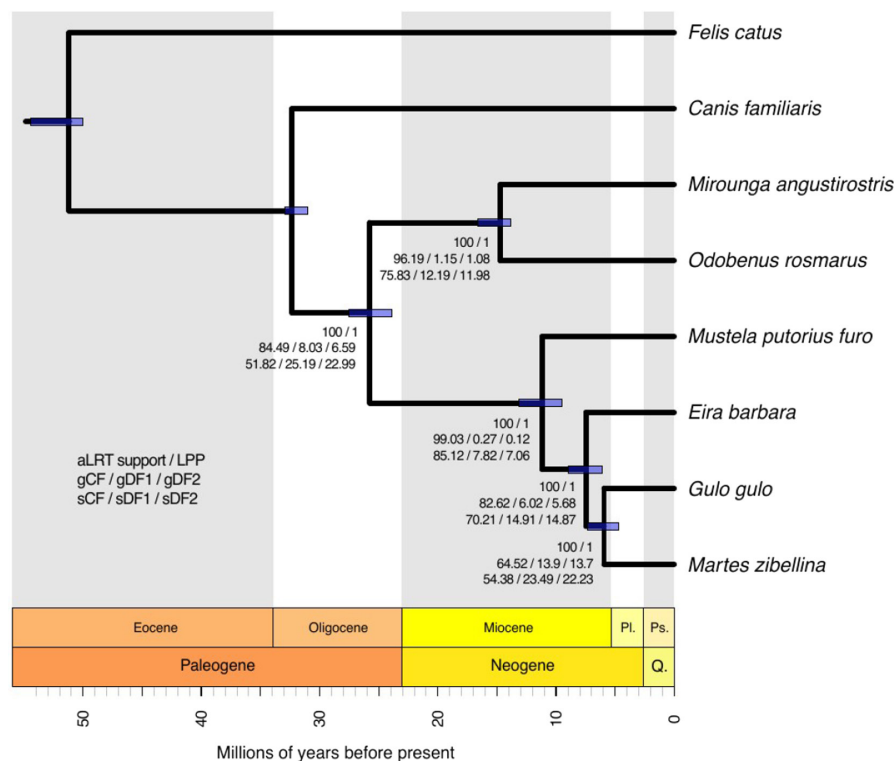
FIGURE 3 Phylogenetic tree and divergence times of Guloninae and five other carnivorans. The mean age of each node is shown, with 95% confidence intervals depicted as purple bars. The gene and site concordance (gCF, sCF) and discordance (gDF, sDF) factors are given. While the concordance factors refer to the portions of the data in agreement with the tree shown, each of the two discordance factors (DF1 and DF2) refer to the support for each of the two other possible alternative quartet resolutions for each branch. Also included are the tree branch supports as calculated using approximate likelihood-ratio tests (aLRT) and local posterior probabilities (LPP)

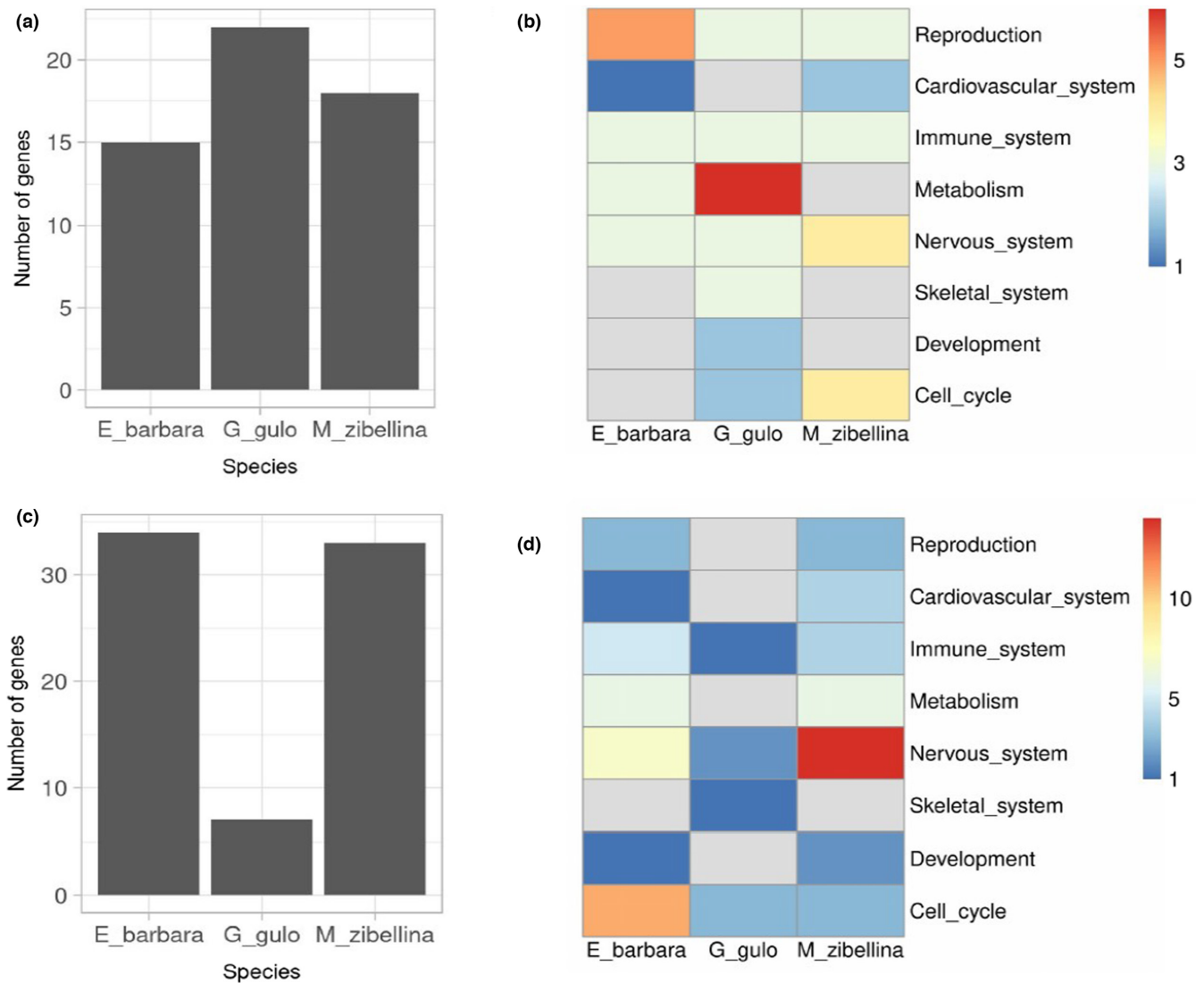## 3.7 | Gene family expansions and contractions

Adaptive divergence between species may also be caused by changes in gene family sizes that occur during genome evolution and are due to gains (expansions) or losses (contractions) of genes or groups of genes (Olson, 1999; Tigano et al., 2020). All species analysed displayed more gene family contractions than expansions, with the wolverine having the highest contraction rate. This is probably an artefact resulting from the fragmented genome assembly of this species (Figure S7). All identified expansions were in the form of gene duplications, with one putative triplication detected in tayra (Table S5B).

Tayra and sable had similar numbers of gene family expansions and contractions (Figure S7): 34 expansions and 169 contractions in tayra, and 33 expansions and 162 contractions in sable. The less contiguous wolverine genome contained seven expansions and 649 contractions (Table S5A,B). Due to the stochastic nature of gene losses and the potential inflation of estimates resulting from different genome assembly contiguities, we focus here on gains of gene copies.

Expanded gene families in the tayra genome are associated with reproduction, metabolism, the nervous and immune system, and cell cycle, among others (Figure 4c,d; gene names, descriptions and functions are given in Table S5B). Of the three reproduction-related genes, *SLC38A2* regulates supply of nutrients for fetal growth through the placenta during the peri-implantation period. The second, *HSD17B10*, is associated with regulation of pregnancy-sustaining steroid hormones, and *RBP2* is involved in retinol binding and vitamin A metabolism, necessary for oogenesis and embryogenesis, as well

as vision. Four genes (*PDHB*, *SH3GLB1*, *SLC35A1*, *N6AMT1*) are involved in metabolic processes, with *N6AMT1* specifically associated with modulation of arsenic-induced toxicity. Four genes (*ATP6V1D*, *DBX2*, *SLC38A1*, *MAPKAPK5*) are associated with cerebral cortex development, synapse formation, visual perception and learning processes. *ANKRD13A* is also associated with vision, more specifically with lens fibre generation and vitamin A metabolism. The olfactory receptor gene *TAAR5* is involved in behavioural responses in mammals, and was duplicated in both tayra and sable. We detected one putative triplication of *FKBP3*, a gene associated with immunoregulation, predominantly of T-cell proliferation. Four additional genes are associated with the innate immune system (*TUFM*, *UBXN6*, *SPON2*, *SERPINB1*). Two genes (*MRPS14* and *MRPS23*) are involved in energy conversion. Two genes (*ATF4* and *ARDI2*) are associated with the cardiovascular system and development, respectively. The rest of the genes are involved in processes related to the cell cycle, and *PRR11* could not be associated with a particular biological process. Among duplications in the tayra, seven were recent duplications, 16 are under relaxed selection and 10 under purifying selection (Table S5B). Gene enrichment analysis revealed an overrepresentation of genes in GO categories associated with metabolism/energy conversion (Table S5C, multiple pathways, $p < .02$), the cardiovascular system (multiple pathways, $p < .02$), the immune system (multiple pathways, $p < .02$) and cell cycle processes (multiple pathways, $p < .02$).

In the wolverine, two duplicated genes are related to the nervous system: *GFRA4* is implicated in motor neuron development and *KCNS1* in regulating mechanical and thermal pain sensitivity. *MTM1* is associated with positive regulation of skeletal muscle tissue growth and *MON1B* is implicated in the immune response to viral

—WILEY—

FIGURE 4 Number of candidate genes and their functional groups. Genes identified from analyses of (a, b) positive selection on single genes (PSG), and (c, d) gene family expansions. Heatmap scale represents the number of genes. Heatmap cells in grey indicate no observations for a given variable

infection. Three duplicated genes are associated with cell cycle processes. Among duplications in the wolverine, one is a recent duplication, one is under relaxed selection and two are under purifying selection (Table S5B). No overrepresentation of GO categories was detected.

In the sable, expansions involve gene families associated with the nervous system, metabolism, angiogenesis, hair follicle development and the immune system, among others (Table S5B). Fourteen genes are associated with the nervous system. Among them, six (*PPA1*, *THOC6*, *SHISAL2A*, *SHISAL1*, *FICD*, *DUSP8*) are involved in neuronal development, two (*SYNGR3*, *TM4SF20*) are associated with locomotion, and two (*MFSD5* and *BICDL2*) with energy regulation and secretion. *TAAR5* is associated with olfaction, *FBXL3* with regulation of the circadian clock and *TIMM10* with hearing. *CD93* is associated with regulation of inflammation in the central nervous system. Six genes are involved with metabolism and energy conversion (*ASB6*,

CRYZL1, *SLC25A10*, *CLDN20*, *RNF186*, *BORCS6*). Three genes (*GPS2*, *BRICD5*, *HCFC1R1*) are associated with the immune system. Two genes, *CDC42* and *TCHHL1*, are implicated in hair-follicle development. Additionally, *CDC42*, a gene coding for a cell division control protein, is also involved in angiogenesis and haematopoiesis, alongside *SLC25A39*, *TNFRSF12A* and *LXN*. Three genes (*MRPL38*, *RPP30*, *TBL3*) are associated with basal cell cycle processes and two genes (*SEPT12*, *CDK2*) with gametogenesis.

Among duplications in the sable, seven were recent duplications, nine are under relaxed selection, 15 are under purifying selection and two are under positive selection (Table S5B). Gene enrichment analysis revealed an overrepresentation of genes in GO categories associated with metabolism/energy conversion (Table S5C; GO:0006839, "Mitochondrial transport," $p = .018$), the nervous system (multiple pathways, $p < .03$) and cell cycle processes (multiple pathways, $p < .03$).

3.8 | Structural variation

SVs modify the structure of chromosomes and can affect gene synteny, repertoire, copy number and/or composition (e.g. gain or loss of exons), create linkage-blocks and modify gene expression (Chiang et al., 2017; Mérot et al., 2020), leading to complex variation in phenotypes and genetic diseases (Weischenfeldt et al., 2013). We investigated four types of SVs (deletions, duplications, insertions, inversions) in the three Guloninae relative to the domestic ferret genome.

We identified the highest number of species-specific SVs in sable (22,979), followed by tayra (8907) and wolverine (264) (Figure 5a). The most abundant SVs detected in all three species are deletions (>50 bp), ranging from 183 species-specific deletions in wolverine to 21,713 in sable. Duplications were the least frequent SV type among the three species (Figure S8A). For all three species, the majority of SVs are located in intergenic regions (>80%), with a smaller proportion found in genic regions, completely or partially overlapping protein-coding genes (untranslated regions, exons, introns). According to Variant Effect Predictor (VEP) classification, SVs impacting genic regions are classified either as high-impact variants or modifiers (McLaren et al., 2016) with putative consequences on gene transcription ranging from transcript truncation to transcript ablation or amplification. The highest number of species-specific genic SVs was detected in tayra, with 330 (3.70% of species-specific SVs), followed by 156 (0.68%) in sable and 53 (20.08%) in wolverine (Figure S8B). Other than the well-documented impact of inversions on intra- and interspecific gene flow (Porubsky et al., 2020; Wellenreuther & Bernatchez, 2018), determining the impact of inversions overlapping large sets of genes is still challenging, as the largest effect is likely to be restricted to genes near SV breakpoints. Therefore, we restricted our examination of gene function to loci affected by deletions, duplications and insertions (Figure 5b; gene names, descriptions and functions are given in Table S6).

In the tayra genome, we observed 14 duplications spanning a combined length of 2.92 Mb, putatively affecting 24 protein-coding genes. Duplicated genes and gene blocks are associated with reproduction, olfaction, metabolism and energy conversion. This included *RNASEH2B*, a gene involved in *in utero* embryo development, and two genes involved in spermatogenesis, *DIAPH3* and *PCNX1*, with the latter an example of a complex SV involving heterozygous duplication and deletion of an exon (SV ~2 kb in length). We detected 212 deletions in the tayra genome in relation to the domestic ferret reference, comprising a total length of 2.08 Mb, and affecting 247 genes, which are associated with reproduction, metabolism/energy conversion, the nervous system and cell cycle processes, among other functional categories (Table S6). Genes involved in placenta development and *in utero* embryogenesis include *HSF1*, *RSPO2* and *DNMT3A*. Additionally, we detected *NLRP1* and *NLRP8*, both associated with pre-implantation development, and highly expressed in oocytes. One short insertion was observed in *LIX1L*, a gene associated with anatomical structure morphogenesis. No overrepresentation of GO categories was detected.

In the wolverine genome, no duplications overlapped genic regions. However, 47 deletions spanning a combined length of 229 kb are putatively associated with transcript truncation or ablation in 48 genes. The majority of affected genes are associated with metabolism/energy conversion, development and basic cell cycle processes. These include *GLUD1*, a gene involved in amino-acid-induced insulin secretion, also found to be affected by a shorter deletion in sable, and *NSDHL*, a gene regulating cholesterol biosynthesis. Additionally, we detected deletions affecting *PARVA*, a gene associated with angiogenesis and smooth muscle cell chemotaxis, and *DNAJC7*, involved in positive regulation of ATPase activity and regulation of cellular response to heat. We also detected one insertion in a gene of unknown function. No overrepresentation of GO categories was detected.

In the sable genome, we detected 11 duplications spanning a combined length of 324 kb, overlapping 16 genes associated with sensory perception, development, the cell cycle and the immune system. The 130 detected deletions (combined length of 408 kb) overlap 125 protein-coding genes associated with reproduction, the immune system, development, metabolism, sensory perception and the cell cycle. Deletions were identified in two genes involved in keratinocyte differentiation, *PPHLN1*, also affected in wolverine, and *IVL*, associated with hair follicle development. Additionally, two short insertions were found in *NCOA4* and *YIPF5*, genes associated with mitochondrial iron homeostasis and protein transport, respectively. Gene enrichment analysis revealed an overrepresentation of genes in GO categories associated with cellular responses to xenobiotic compounds (Table S6A; multiple pathways, $p < .05$).

4 | DISCUSSION

Here, we present a highly contiguous genome for the tayra (*Eira barbara*). Contiguity of the assembly and its gene completeness are similar to or higher than those of other carnivoran species using the same sequencing approach (Armstrong et al., 2019; Etherington et al., 2020; Kim et al., 2020), confirming the utility of linked reads for assembly of mammal genomes.

Phylogenomic relationships among the mustelids resulted in a tree topology and divergence time estimates in agreement with previous studies using fewer loci (Koepfli et al., 2008; Koepfli et al., 2018; Li et al., 2014; Sato et al., 2012). We estimated the split between *Mustela* and Guloninae occurred 11.2 Ma (HPDI 13.1–9.5 Ma), followed by the split between *Eira* and the *Gulo–Martes* group 7.5 Ma (HPDI 9–6.1 Ma), and the split between *Gulo* and *Martes* at 5.9 Ma (HPDI 7.4–4.7 Ma).

Perhaps unsurprisingly, we observed different historical trends in effective population size among the three Guloninae. They differ markedly in ecology, and it is not unexpected that climatic and environmental changes (affecting, for example, habitat, ecological competition, prey and pathogens) also differentially impacted tayra, wolverine and sable populations. Consistent with previous

(a)

(b)
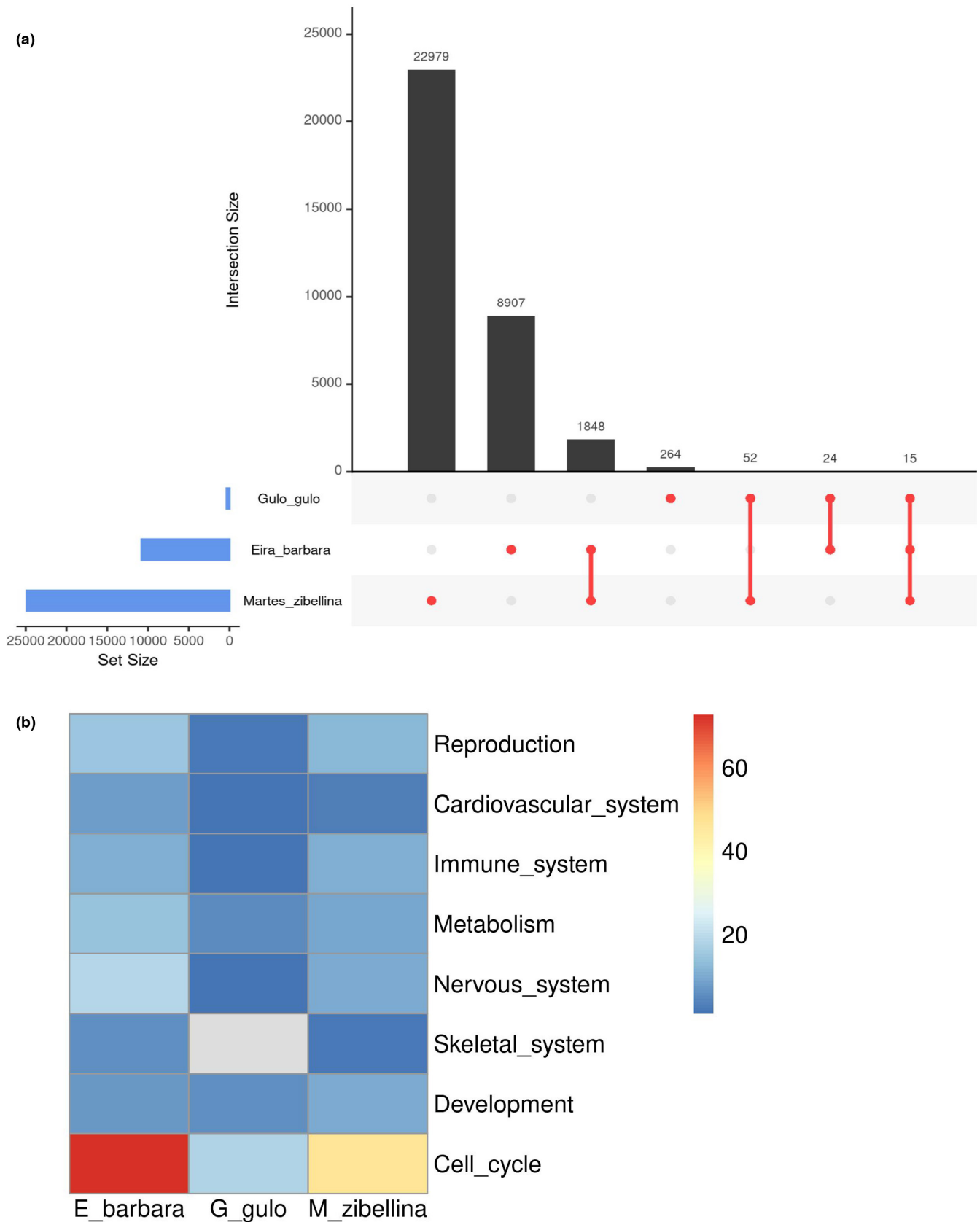
FIGURE 5 Structural variants detected in gulonine species. (a) Shared and species-specific structural variants detected in wolverine (*Gulo gulo*), tayra (*Eira barbara*) and sable (*Martes zibellina*). (b) Functional groups of genes affected by species-specific structural variants in three gulonine species (SV types: DEL, DUP, INS). Heatmap scale represents the number of genes. Heatmap cells in grey indicate no observations for a given variable

work (Ekblom et al., 2018), we observed low recent effective population size in wolverines, and a concomitant low genome-wide heterozygosity.

Contrary to the findings by Weissensteiner et al. (2020) in corvids, we did not observe a positive relationship between variation at the nucleotide level (heterozygous SNPs) and variation at the structural level (heterozygous SVs) within the gulonine species. The tayra displayed the highest nucleotide diversity (1.89 SNPs per kbp), but only the second highest amount of heterozygous SVs (2,543, 23.6% of the total SVs, Figure S9). The sable had the second highest nucleotide diversity (1.44 SNPs per kbp), but the highest number of heterozygous SVs (14,823, 59.5% of the total). The wolverine displayed the lowest variation for both (0.28 SNPs per kbp, and 153 or 43.1% heterozygous SVs in total). It is known that SV calling using short-read data can miss a large number of SVs (Ebert et al., 2021). The fact that we did not detect a positive correlation between variation at the nucleotide and structural level, as would be expected if diversity of SNPs and SVs are correlated with population size, may result from our SV analysis relying on short-read data only. Weissensteiner et al. (2020), who did report a positive correlation between SNP and SV diversity, performed long-read-based SV typing.

Assessment of variation among genome assemblies of closely related species is also strongly impacted by the contiguity and completeness of the analysed assemblies (Gurevich et al., 2013; Totikov et al., 2021). This needs to be accounted for when examining variation among discontiguous genome assemblies. Here, the low contiguity of the wolverine assembly has probably impacted the number of PSGs and gene family expansions/contractions detected. Additionally, the use of multiple, short insert size libraries sequenced at low coverage for the wolverine (Ekblom et al., 2018) has probably resulted in decreased SV detectability. We would thus argue that future comparative genomics studies of Guloninae may benefit from improving the contiguity and completeness of the wolverine genome.

4.1 | Adaptive genomic variation

Among positively selected genes, gene family expansions and coding regions impacted by SVs, we found numerous candidate loci that may be associated with species-specific traits in Guloninae.

For example, the tayra has an atypical reproductive strategy among Guloninae, namely aseasonal breeding. Among the 23 genes associated with reproduction in tayra (Figure 6a), 10 were pregnancy-related (two PSGs, two GF, six SVs), which may be linked to this species' reproductive strategy. In the hypercarnivorous wolverine, we did not observe any candidate loci associated with carbohydrate metabolism ("omnivorous diet," Figure 6b), while several were detected in the omnivorous tayra (one PSG, two GF, three SVs). However, we did observe seven genes (six PSGs, one GF) associated with body condition in wolverines, which may reflect this species' adaptive response to unfavourable environmental conditions in its circumpolar habitat. We discuss candidate loci in the context of the three species' ecology in more detail below.

We note that in two analyses (PSGs and gene family evolution), we only considered variation in single-copy orthologues, not in the entire gene repertoire of these species. Thus, our results are probably only an incomplete reflection of the genes involved in these traits.

4.2 | Seasonal breeders in the north palaearctic: wolverine and sable

Obligate embryonic diapause or delayed implantation of the blastocyst is a widespread reproductive strategy among seasonally breeding mustelids and other carnivorans. For example, wolverines and sables delay implantation for several months (Mead, 1981; Svishcheva & Kashtanov, 2011). Conspecific encounters are rare (Inman et al., 2012; Kashtanov et al., 2015), and thus induced ovulation during encounters is advantageous (Larivière & Ferguson, 2003). Previous studies in mink showed that increased levels of vascular endothelial growth factors (VEGFs) and their receptors correlate with the implantation process (Lopes et al., 2003). *VEGFC*, primarily associated with angiogenesis and regulation of permeability of blood vessels during embryogenesis, was positively selected in sable, suggesting its possible involvement in embryo implantation regulation in this species. In wolverine, we detected signals of positive selection in *ANAPC7*, a gene involved in progesterone-mediated oocyte maturation and release from cell arrest prior to fertilization (Papin et al., 2004; Reis et al., 2006), that may have a role in increasing progesterone secretion and renewed embryonic development, as observed in skunks and mink (Mead, 1989).

Changes in testicular activity and spermatogenesis also correlate strongly with season (mink: Blottner et al., 2006, lynx: Jewgenow et al., 2006). In the wolverine, positively selected genes involved in spermatogenesis included *IZUMO3*, essential for gamete fusion during fertilization (Ellerman et al., 2009), and *RNF212B*, critical for crossing over in gametes (Reynolds et al., 2013). In sable, candidate genes involved in spermatogenesis were *UBQLNL* and *SEPT12*, with the latter also being duplicated. Furthermore, *MEIKIN* and *CDK2*, both involved in meiosis, show signals of positive selection and rapid evolution through gene family expansion, respectively.

Seasonal breeding in many mammals is largely under photoperiod regulation, suggesting that the circadian system plays an important role in this reproductive strategy. *FBXL3*, associated with maintenance of circadian clock oscillation in mammals (Shi et al., 2013; Siepka et al., 2007), is duplicated in sable.

4.3 | Aseasonal breeder in the neotropic: tayra

In tropical regions, reproduction does not depend on season as environmental conditions are relatively stable throughout the year (McNutt et al., 2019). Tayras are aseasonal breeders with multiple oestrous cycles per year (Proulx & Aubry, 2017) and do not exhibit embryonic diapause (Poglayen-Neuwall et al., 1989). The tayra
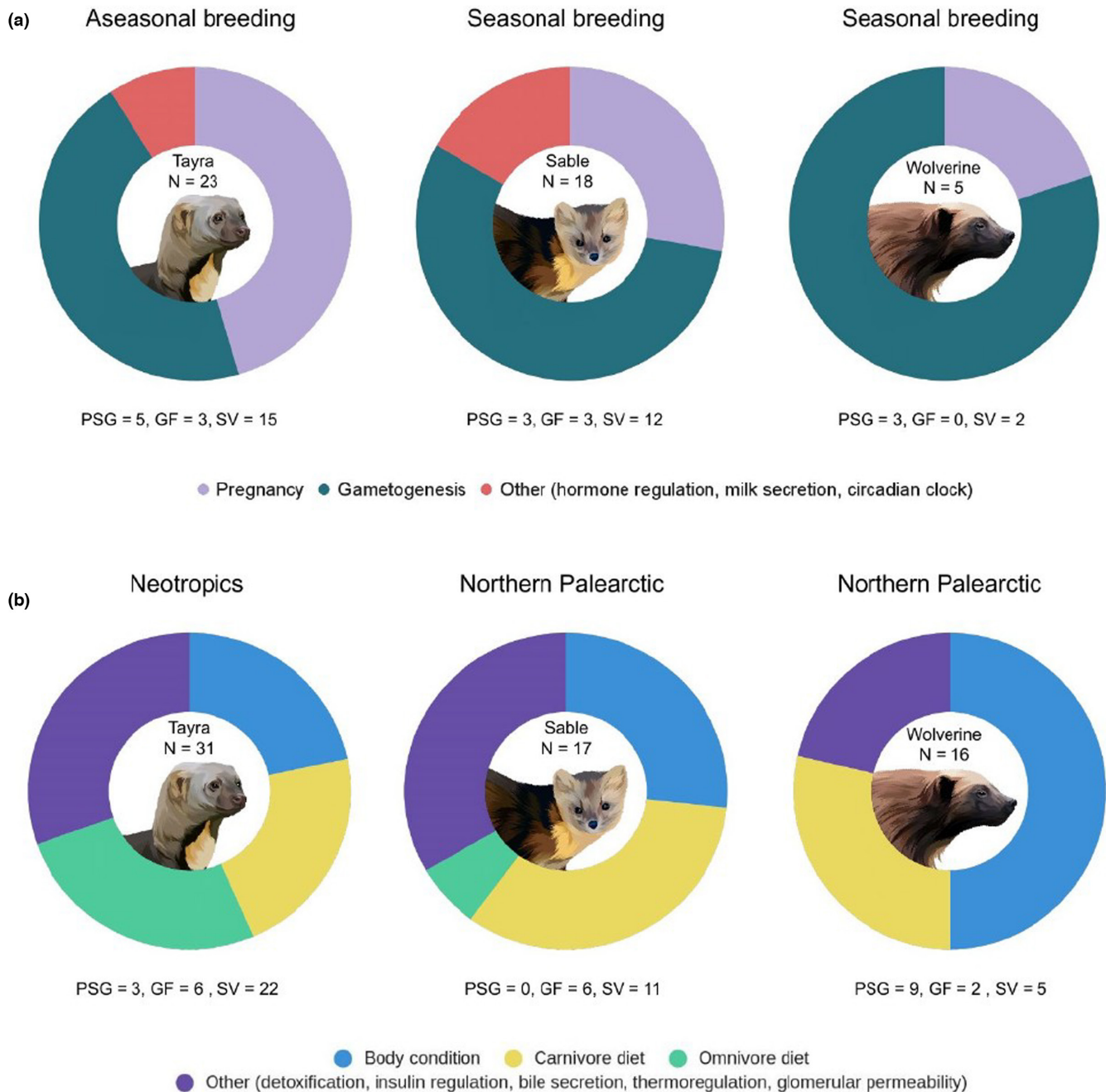
FIGURE 6 Summary of functional categories of (a) reproduction and (b) metabolism-related genes derived from analyses of positively selected genes (PSG), gene family expansion (GF) and structural variation (SV). N represents the total number of detected genes. Vector graphics of species are created based on royalty-free images (Source: Shutterstock)

represents the most basal taxon of the Guloninae and is an exception regarding its reproductive strategy.

We detected candidate genes in tayra that are related to pregnancy, and thus potentially to aseasonal breeding in this species. *ETV2* and *MUC15*, both under positive selection, are associated with placental and embryo development, and regulation of implantation (Poon et al., 2014; Singh et al., 2019). *SLC38A2*, which is duplicated in tayra, is upregulated in the pre-implantation period (Forde et al., 2014) and during late gestation, maintaining fetal growth when maternal growth is restricted by undernutrition

(Coan et al., 2010). *HSD17B10*, duplicated in tayra, is highly expressed in fetal and maternal livers, maintains pregnancy and provides protection against excitotoxicity (Hill et al., 2011). *RBP2*, also duplicated in tayra, regulates retinoids during oogenesis and embryogenesis, and positively impacts oocyte maturation in mice, cattle, pigs and sheep (Brown et al., 2003; Harney et al., 1993). Furthermore, six genes involved in placental development, implantation and embryogenesis (*HSF1*, *RSPO2*, *NLRP1*, *NLRP8*, *RNASEH2B* and *DNMT3A*) have been affected by partial deletions or duplications in tayra, raising the possibility of further

modification (e.g., functional or regulatory) of these pregnancy-related genes. Partial deletions or duplications overlapping one or more exons in protein-coding genes impact RNA splicing patterns and subsequently protein functions. They lead to production of protein isoforms with different structural and functional properties, or modulate mRNA translational efficiency, or lastly, lead to pseudogenization of a gene (Wang et al., 2015; Xing & Lee, 2006).

4.4 | Resource availability in the northern Palaearctic: wolverine and sable

Surviving the winter is challenging for nonhibernating northern palearctic species and requires specific mechanisms to cope with adverse temperatures and food scarcity. Thus, efficient storage and mobilization of fat is very important in low-productivity environments (Inman et al., 2012). Three PSGs detected in the wolverine are involved in formation of adipose tissue, *MTPAP*, *OIP5* and *ZADH2* (Han et al., 2012; Inoue et al., 2014; Yu et al., 2013) and selective fatty acid mobilization stimulated by fasting periods (Inman et al., 2012; Krebs et al., 2004), as observed in mink (Nieminen et al., 2006) and raccoon dog (Mustonen et al., 2007).

One of the responses to prolonged periods of nutrient deprivation and extreme environmental conditions is suppressed bone resorption and formation (Lennox & Goodship, 2008; McGee-Lawrence et al., 2015). While the control of autophagy is important for the survival of blastocysts during delayed implantation (Lee et al., 2011; Lim & Song, 2014), it is also very important in maintaining bone homeostasis (DeSelm et al., 2011; Montaseri et al., 2020). It is thus of note that genes involved in bone mass regulation, resorption (*PPP1R18*, *TMEM38B*) and autophagy (*NBR1*) are under positive selection in wolverines. We also detected a duplication of the muscle growth-regulating gene *MTM1*. While a lack of *MTM1* will lead to muscle hypotrophy through unbalanced autophagy in humans and mice (Al-Qusairi et al., 2013), a gene duplication may facilitate muscle growth or counteract muscle reduction.

In sable, fatty acids are mobilized from fat deposits (Nieminen & Mustonen, 2007), and we observed duplications of *ASB6*, *SLC25A10*, *RNF186* and *BORCS6*, which regulate fat storage and response to nutrient availability (Mizuarai et al., 2005; Okamoto et al., 2020; Schweitzer et al., 2015; Wilcox et al., 2004). The partial deletions we detected in *APOD*, *PDHB*, *LDLR* and *CERS5*, all associated with lipoprotein metabolism (Carmo et al., 2009; Gosejacob et al., 2016; Serão et al., 2011; Tavori et al., 2015), indicate modification of genes in pathways associated with energy conservation in this species.

We observed partial deletions in *DNAJC7* in both sable and wolverine, indicating independent modification of this thermoregulation gene (Sonna et al., 2002) in gulonines inhabiting colder environments. Another gene in which we detected independent partial deletions in sable and wolverine is *GLUD1*, which regulates insulin homeostasis (Fahien & Macdonald, 2011). Modification of this gene may impact "adaptive fasting" in these species, an adaptation to prolonged periods of nutrient deprivation observed in several carnivorans (Martinez & Ortiz, 2017; Viscarra et al., 2013).

Sables are famous for their dense fur, and we observed two duplications that may be linked to this trait: *TCHHL1*, involved in hair morphogenesis (Wu et al., 2011), and *CDC42*, required for differentiation of hair follicle progenitor cells (Wu et al., 2006).

4.5 | Resource availability in the Neotropics: tayra

Tayras exploit diverse food sources and experience relatively stable resource availability all year round (Zhou et al., 2011). Shifts in dietary preferences have been linked to positive selection in single genes (Kosiol et al., 2008) and to copy number variation in metabolism-related gene families in mammals (Hecker et al., 2019; Rinker et al., 2019). In tayra, we found candidate genes associated with fructose metabolism, which may be associated with the addition of fruits and honey to this species' diet. For example, *UOX*, involved in regulation of purine metabolism and conversion of fructose to fat (Johnson & Andrews, 2010), and *DERA*, associated with catabolic processes, were both under positive selection in tayra, and part of significantly overrepresented GO categories in this species.

High rates of lineage-specific variation in gene family size, especially those families involved in immune response or detoxification of xenobiotic molecules (Thomas, 2007), are probably associated with environmental changes during speciation (Lynch & Conery, 2000; Zhang, 2003). We found a duplication of *N6AMT1*, which is associated with conversion of an arsenic metabolite, monomethylarsonous acid, to the less toxic dimethylarsonic acid (Ren et al., 2011). Arsenic with geothermal origins (e.g., volcanic activity) is common in Latin America, where it represents a severe threat to public health and the livelihoods of millions of people, with chronic exposure leading to various diseases (Morales-Simfors et al., 2020; Zhang et al., 2015). This duplication may represent an adaptation of tayra to this xenobiotic compound.

Finally, we also found candidate genes associated with lens fibre formation and retinal vascularization in tayra, including gene expansions of *ANKRD13A* (Avellino et al., 2013) and *RBP2* (D'Ambrosio et al., 2011). It has been suggested that tayras detect prey primarily by smell, as their eyesight has been described as being relatively poor (Defler, 1980; Wilson & Mittermeier, 2009). However, this has not been experimentally tested, and it is somewhat contradictory to the observed behaviour of caching of unripe but mature stages of both native and non-native fruits (Soley & Alvarado-Díaz, 2011). As tayras inhabit (sub)tropical forests, where mammals rely on vision, alongside olfaction, to forage and avoid potentially poisonous prey (Alatalo & Mappes, 1996; Nelson et al., 2011; Webb et al., 2008), we suggest that "poor" eyesight would not be advantageous, as this would impede recognition of noxious prey displaying conspicuous coloration (Blount et al., 2009). It may thus be appropriate to revisit tayras' visual acuity.

4.6 | Conclusion and future outlook

Mustelids are a remarkable example of adaptive radiation, and we show how positively selected loci, changes in gene family size and SVs have shaped genomes in this diverse taxonomic group. We demonstrated that, in particular, the latter two sources of variation contribute many loci potentially involved in adaptive genomic evolution. In the past, these types of genomic variation were often not considered in comparative genomic studies of nonmodel species, even though they encompass more nucleotides than SNPs. To fully explore the impact of different types of genomic variants on phenotypic variation, gene expression data would be necessary. Comparative analysis of gene expression patterns and elucidating protein interactions and pathways is a domain of functional genomics, and was unfortunately outside the scope of our study.

The mustelid subfamily Guloninae includes three monotypic genera (*Eira*, *Gulo* and *Pekania*) as well as the martens (eight *Martes* species). A feasible short-term goal regarding future genomics studies of this subfamily is the generation of reference genomes for all remaining Guloninae, which is a goal of the *Martes* Genome Consortium, launched in 2018. Additionally, existing reference genomes may be improved in contiguity using, for example, Hi-C approaches (e.g., Dudchenko et al., 2017; DNAzoo.org). This will be a strong foundation for both inter- and intraspecific genomics studies of Guloninae, which includes species of conservation concern (wolverine and Nilgiri martens: "vulnerable" on the IUCN red list), species that hybridize in nature (e.g., European pine martens and sables; Davison et al., 2001; Kassal & Sidorov, 2013), and species characterized by convergent evolution of ecological adaptations (e.g., delayed implantation, seasonal moulting, sociality, scent glands).

AUTHOR CONTRIBUTIONS
L.D. conceived the study, conducted genome assembly, gene family evolution and structural variation analysis, interpreted the data, and wrote the manuscript. A.B. and S.J. conducted positive selection analysis, and interpreted the data. P.D. carried out demographic history reconstruction and data interpretation. D.A.D. designed and performed phylogenomic analysis and molecular dating, and wrote the manuscript. J.H.G. conducted repetitive elements analysis and interpreted the data. S.K., A.T. and A.T. performed reference-based scaffolding, alignment to pseudochromosome assemblies, sex verification and nucleotide diversity assessment, interpreted the data and wrote the manuscript. K.P.K. advised on comparative genomic analyses, and edited the manuscript. D.M. supervised and performed gene family evolution analysis, and advised on other comparative genomic analyses. M.P. conducted whole genome sequencing and sequencing data interpretation. J.F. and D.W.F. conceived the study, interpreted the data, and wrote and edited the manuscript. All authors have reviewed and approved the manuscript.

OPEN RESEARCH BADGES

This article has been awarded Open Data Badges. All materials and data are publicly accessible via the Open Science Framework at https://doi.org/10.5061/dryad.xgxd254hz and https://doi.org/10.5281/zenodo.6320689.

DATA AVAILABILITY STATEMENT
The tayra principal genome assembly and raw sequencing reads have been deposited under the NCBI BioProject ID: PRJNA732553, and the alternative assembly can be accessed under BioProject ID: PRJNA732552. The vcf files with variant calling data are available at Dryad (https://doi.org/10.5061/dryad.xgxd254hz), and scripts at Zenodo (https://doi.org/10.5281/zenodo.6320689). All data generated or analysed during this study are included in this published article and its Supporting Information files.

ORCID
Lorena Derežanin https://orcid.org/0000-0002-0707-573X
Pavel Dobrynin https://orcid.org/0000-0001-6995-5620

REFERENCES
Abduriyim, S., Nishita, Y., Abramov, A. V., Solovyev, V. A., Saveljev, A. P., Kosintsev, P. A., Kryukov, A. P., Raichev, E., Väinölä, R., Kaneko, Y., & Masuda, R. (2019). Variation in pancreatic amylase gene copy number among Eurasian badgers (Carnivora, Mustelidae, Meles) and its relationship to diet. *Journal of Zoology*, *308*(1), 28–36.

Alatalo, R. V., & Mappes, J. (1996). Tracking the evolution of warning signals. *Nature*, *382*(6593), 708–710.

Alonge, M., Soyk, S., Ramakrishnan, S., Wang, X., Goodwin, S., Sedlazeck, F. J., Lippman, Z. B., & Schatz, M. C. (2019). RaGOO: fast and accurate reference-guided scaffolding of draft genomes. *Genome Biology*, *20*(1), 224. https://doi.org/10.1186/s13059-019-1829-6

Al-Qusairi, L., Prokic, I., Amoasii, L., Kretz, C., Messaddeq, N., Mandel, J.-L., & Laporte, J. (2013). Lack of myotubularin (MTM1) leads to muscle hypotrophy through unbalanced regulation of the autophagy and ubiquitin-proteasome pathways. *FASEB Journal*, *27*(8), 3384–3394. https://doi.org/10.1096/fj.12-220947

Angelis, K., & Dos Reis, M. (2015). The impact of ancestral population size and incomplete lineage sorting on Bayesian estimation of species divergence times. *Current Zoology*, *61*(5), 874–885.

Anisimova, M., & Gascuel, O. (2006). Approximate likelihood-ratio test for branches: A fast, accurate, and powerful alternative. *Systematic Biology*, *55*(4), 539–552.

Armstrong, E. E., Taylor, R. W., Prost, S., Blinston, P., van der Meer, E., Madzikanda, H., Mufute, O., Mandisodza-Chikerema, R., Stuelpnagel, J., Sillero-Zubiri, C., & Petrov, D. (2019). Cost-effective assembly of the African wild dog (*Lycaon pictus*) genome using linked reads. *GigaScience*, 8(2), https://doi.org/10.1093/gigascience/giy124

Avellino, R., Carrella, S., Pirozzi, M., Risolino, M., Salierno, F. G., Franco, P., Stoppelli, P., Verde, P., Banfi, S., & Conte, I. (2013). miR-204 targeting of Ankrd13A controls both mesenchymal neural crest and lens cell migration. *PLoS One*, 8(4), e61099. https://doi.org/10.1371/journal.pone.0061099

Barnett, R., Westbury, M. V., Sandoval-Velasco, M., Vieira, F. G., Jeon, S., Zazula, G., Martin, M. D., Ho, S. Y. W., Mather, N., Gopalakrishnan, S., Ramos-Madrigal, J., de Manuel, M., Zepeda-Mendoza, M. L., Antunes, A., Baez, A. C., De Cahsan, B., Larson, G., O'Brien, S. J., Eizirik, E., … Gilbert, M. T. P. (2020). Genomic adaptations and evolutionary history of the extinct scimitar-toothed cat, *Homotherium latidens*. *Current Biology*, 30(24), 5018–5025.e5. https://doi.org/10.1016/j.cub.2020.09.051

Beichman, A. C., Koepfli, K.-P., Li, G., Murphy, W., Dobrynin, P., Kilver, S., Tinker, M. T., Murray, M. J., Johnson, J., Lindblad-Toh, K., Karlsson, E. K., Lohmueller, K. E., & Wayne, R. K. (2019). Aquatic adaptation and depleted diversity: a deep dive into the genomes of the sea otter and giant otter. *Molecular Biology and Evolution*, 36(12), 2631–2655. https://doi.org/10.1093/molbev/msz101

Blottner, S., Schön, J., & Jewgenow, K. (2006). Seasonally activated spermatogenesis is correlated with increased testicular production of testosterone and epidermal growth factor in mink (*Mustela vison*). *Theriogenology*, 66(6–7), 1593–1598. https://doi.org/10.1016/j.theriogenology.2006.01.041

Blount, J. D., Speed, M. P., Ruxton, G. D., & Stephens, P. A. (2009). Warning displays may function as honest signals of toxicity. *Proceedings Biological Sciences*, 276(1658), 871–877.

Broad Institute (2019). Picard Toolkit. GitHub Repository. https://broadinstitute.github.io/picard/

Brown, J. A., Eberhardt, D. M., Schrick, F. N., Roberts, M. P., & Godkin, J. D. (2003). Expression of retinol-binding protein and cellular retinol-binding protein in the bovine ovary. *Molecular Reproduction and Development*, 64(3), 261–269. https://doi.org/10.1002/mrd.10225

Buckley, R. M., Davis, B. W., Brashear, W. A., Farias, F. H. G., Kuroki, K., Graves, T., Hillier, L. W., Kremitzki, M., Li, G., Middleton, R. P., Minx, P., Tomlinson, C., Lyons, L. A., Murphy, W. J., & Warren, W. C. (2020). A new domestic cat genome assembly based on long sequence reads empowers feline genomic medicine and identifies a novel gene for dwarfism. *PLoS Genetics*, 16(10), e1008926. https://doi.org/10.1371/journal.pgen.1008926

Cahill, J. A., Soares, A. E. R., Green, R. E., & Shapiro, B. (2016). Inferring species divergence times using pairwise sequential Markovian coalescent modelling and low-coverage genomic data. *Philosophical Transactions of the Royal Society B: Biological Sciences*, 371(1699), https://doi.org/10.1098/rstb.2015.0138

Carmo, S. D., Fournier, D., Mounier, C., & Rassart, E. (2009). Human apolipoprotein D overexpression in transgenic mice induces insulin resistance and alters lipid metabolism. *American Journal of Physiology-Endocrinology and Metabolism*, 296(4), E802–E811. https://doi.org/10.1152/ajpendo.90725.2008

Catanach, A., Crowhurst, R., Deng, C., David, C., Bernatchez, L., & Wellenreuther, M. (2019). The genomic pool of standing structural variation outnumbers single nucleotide polymorphism by threefold in the marine teleost *Chrysophrys auratus*. *Molecular Ecology*, 28(6), 1210–1223.

Cavagna, P., Menotti, A., & Stanyon, R. (2000). Genomic homology of the domestic ferret with cats and humans. *Mammalian Genome: Official Journal of the International Mammalian Genome Society*, 11(10), 866–870. https://doi.org/10.1007/s003350010172

Chang, J.-M., Di Tommaso, P., & Notredame, C. (2014). TCS: a new multiple sequence alignment reliability measure to estimate alignment accuracy and improve phylogenetic tree reconstruction. *Molecular Biology and Evolution*, 31(6), 1625–1637. https://doi.org/10.1093/molbev/msu117

Chen, X., Schulz-Trieglaff, O., Shaw, R., Barnes, B., Schlesinger, F., Källberg, M., Cox, A. J., Kruglyak, S., & Saunders, C. T. (2016). Manta: rapid detection of structural variants and indels for germline and cancer sequencing applications. *Bioinformatics*, 32(8), 1220–1222. https://doi.org/10.1093/bioinformatics/btv710

Chiang, C., Layer, R. M., Faust, G. G., Lindberg, M. R., Rose, D. B., Garrison, E. P., Marth, G. T., Quinlan, A. R., & Hall, I. M. (2015). SpeedSeq: ultra-fast personal genome analysis and interpretation. *Nature Methods*, 12(10), 966–968. https://doi.org/10.1038/nmeth.3505

Chiang, C., Scott, A. J., Davis, J. R., Tsang, E. K., Li, X., Kim, Y., Hadzic, T., Damani, F. N., Ganel, L., Montgomery, S. B., Battle, A., Conrad, D. F., & Hall, I. M. (2017). The impact of structural variation on human gene expression. *Nature Genetics*, 49(5), 692–699. https://doi.org/10.1038/ng.3834

Coan, P. M., Vaughan, O. R., Sekita, Y., Finn, S. L., Burton, G. J., Constancia, M., & Fowden, A. L. (2010). Adaptations in placental phenotype support fetal growth during undernutrition of pregnant mice. *The Journal of Physiology*, 588(Pt 3), 527–538. https://doi.org/10.1113/jphysiol.2009.181214

Copeland, J. P., & Kucera, T. E. (1997). Wolverine (*Gulo gulo*). In: J. E. Harris, & C. V. Ogan, eds. *Mesocarnivores of Northern California: Biology, management, and survey techniques, workshop manual.* Humboldt State Univ. and the Wildlife Society, California North Coast Chapter, 127 p

D'Ambrosio, D. N., Clugston, R. D., & Blaner, W. S. (2011). Vitamin A metabolism: An update. *Nutrients*, 3(1), 63–103. https://doi.org/10.3390/nu3010063

Davison, A., Birks, J. D., Brookes, R. C., Messenger, J. E., & Griffiths, H. I. (2001). Mitochondrial phylogeography and population history of pine martens *Martes martes* compared with polecats *Mustela putorius*. *Molecular Ecology*, 10(10), 2479–2488. https://doi.org/10.1046/j.1365-294X.2001.01381.x

Defler, T. R. (1980). Notes on interactions between the Tayra (*Eira barbara*) and the white-fronted capuchin (*Cebus albifrons*). *Journal of Mammalogy*, 61(1), 156. https://doi.org/10.2307/1379979

DeSelm, C. J., Miller, B. C., Zou, W., Beatty, W. L., van Meel, E., Takahata, Y., Klumperman, J., Tooze, S. A., Teitelbaum, S. L., & Virgin, H. W. (2011). Autophagy proteins regulate the secretory component of osteoclastic bone resorption. *Developmental Cell*, 21(5), 966–974. https://doi.org/10.1016/j.devcel.2011.08.016

Dobrynin, P., Liu, S., Tamazian, G., Xiong, Z., Yurchenko, A. A., Krasheninnikova, K., Kliver, S., Schmidt-Küntzel, A., Koepfli, K.-P., Johnson, W., Kuderna, L. F. K., García-Pérez, R., Manuel, M. D., Godinez, R., Komissarov, A., Makunin, A., Brukhin, V., Qiu, W., Zhou, L., … O'Brien, S. J. (2015). Genomic legacy of the African cheetah, *Acinonyx jubatus*. *Genome Biology*, 16, 277. https://doi.org/10.1186/s13059-015-0837-4

Dudchenko, O., Batra, S. S., Omer, A. D., Nyquist, S. K., Hoeger, M., Durand, N. C., Shamim, M. S., Machol, I., Lander, E. S., Aiden, A. P., & Aiden, E. L. (2017). De novo assembly of the *Aedes aegypti* genome using Hi-C yields chromosome-length scaffolds. *Science*, 356(6333), 92–95.

Dudchenko, O., Shamim, M. S., Batra, S. S., Durand, N. C., Musial, N. T., Mostofa, R., Pham, M., St Hilaire, B. G., Yao, W., Stamenova, E., Hoeger, M., Nyquist, S. K., Korchina, V., Pletch, K., Flanagan, J. P., Tomaszewicz, A., McAloose, D., Estrada, C. P., Novak, B. J., Aiden, E. L. (2018). The Juicebox Assembly Tools module facilitates de novo assembly of mammalian genomes with chromosome-length scaffolds for under $1000 (p. 254797). https://doi.org/10.1101/254797

Ekblom, R., Brechlin, B., Persson, J., Smeds, L., Johansson, M., Magnusson, J., Flagstad, Ø., & Ellegren, H. (2018). Genome sequencing and

conservation genomics in the Scandinavian wolverine population. *Conservation Biology: the Journal of the Society for Conservation Biology*, 32(6), 1301–1312. https://doi.org/10.1111/cobi.13157

Ellerman, D. A., Pei, J., Gupta, S., Snell, W. J., Myles, D., & Primakoff, P. (2009). Izumo is part of a multiprotein family whose members form large complexes on mammalian sperm. *Molecular Reproduction and Development*, 76(12), 1188–1199. https://doi.org/10.1002/mrd.21092

Etherington, G. J., Heavens, D., Baker, D., Lister, A., McNelly, R., Garcia, G., Clavijo, B., Macaulay, I., Haerty, W., & Di Palma, F. (2020). Sequencing smart: De novo sequencing and assembly approaches for a non-model mammal. *GigaScience*, 9(5), https://doi.org/10.1093/gigascience/giaa045

Fahien, L. A., & Macdonald, M. J. (2011). The complex mechanism of glutamate dehydrogenase in insulin secretion. *Diabetes*, 60(10), 2450–2454. https://doi.org/10.2337/db10-1150

Flynn, J. M., Hubley, R., Goubert, C., Rosen, J., Clark, A. G., Feschotte, C., & Smit, A. F. (2020). RepeatModeler2 for automated genomic discovery of transposable element families. *Proceedings of the National Academy of Sciences of the United States of America*, 117(17), 9451–9457. https://doi.org/10.1073/pnas.1921046117

Forde, N., Simintiras, C. A., Sturmey, R., Mamo, S., Kelly, A. K., Spencer, T. E., Bazer, F. W., & Lonergan, P. (2014). Amino acids in the uterine luminal fluid reflects the temporal changes in transporter expression in the endometrium and conceptus during early pregnancy in cattle. *PLoS One*, 9(6), e100010. https://doi.org/10.1371/journal.pone.0100010

Frith, M. C., & Kawaguchi, R. (2015). Split-alignment of genomes finds orthologies more accurately. *Genome Biology*, 16, 106. https://doi.org/10.1186/s13059-015-0670-9

Ge, S. X., Jung, D., & Yao, R. (2020). ShinyGO: a graphical gene-set enrichment tool for animals and plants. *Bioinformatics*, 36(8), 2628–2629. https://doi.org/10.1093/bioinformatics/btz931

Gosejacob, D., Jäger, P. S., Vom Dorp, K., Frejno, M., Carstensen, A. C., Köhnke, M., Degen, J., Dörmann, P., & Hoch, M. (2016). Ceramide synthase 5 is essential to maintain C16:0-ceramide pools and contributes to the development of diet-induced obesity. *Journal of Biological Chemistry*, 291(13), 6989–7003. https://doi.org/10.1074/jbc.M115.691212

Gurevich, A., Saveliev, V., Vyahhi, N., & Tesler, G. (2013). QUAST: quality assessment tool for genome assemblies. *Bioinformatics*, 29(8), 1072–1075. https://doi.org/10.1093/bioinformatics/btt086

Han, M. V., Thomas, G. W. C., Lugo-Martinez, J., & Hahn, M. W. (2013). Estimating gene gain and loss rates in the presence of error in genome assembly and annotation using CAFE 3. *Molecular Biology and Evolution*, 30(8), 1987–1997. https://doi.org/10.1093/molbev/mst100

Han, X., Jiang, T., Yu, L., Zeng, C., Fan, B., & Liu, B. (2012). Molecular characterization of the porcine MTPAP gene associated with meat quality traits: chromosome localization, expression distribution, and transcriptional regulation. *Molecular and Cellular Biochemistry*, 364(1–2), 173–180. https://doi.org/10.1007/s11010-011-1216-4

Harney, J. P., Ott, T. L., Geisert, R. D., & Bazer, F. W. (1993). Retinol-binding protein gene expression in cyclic and pregnant endometrium of pigs, sheep, and cattle. *Biology of Reproduction*, 49(5), 1066–1073.

Hecker, N., Sharma, V., & Hiller, M. (2019). Convergent gene losses illuminate metabolic and physiological changes in herbivores and carnivores. *Proceedings of the National Academy of Sciences of the United States of America*, 116(8), 3036–3041. https://doi.org/10.1073/pnas.1818504116

Heldstab, S. A., Müller, D. W. H., Graber, S. M., Bingaman Lackey, L., Rensch, E., Hatt, J.-M., Zerbe, P., & Clauss, M. (2018). Geographical origin, delayed implantation, and induced ovulation explain reproductive seasonality in the Carnivora. *Journal of Biological Rhythms*, 33(4), 402–419. https://doi.org/10.1177/0748730418773620

Hill, M., Pařízek, A., Kancheva, R., & Jirásek, J. E. (2011). Reduced progesterone metabolites in human late pregnancy. *Physiological Research*, 60(2), 225–241. https://doi.org/10.33549/physiolres.932077

Hron, T., Elleder, D., & Gifford, R. J. (2019). Deltaretroviruses have circulated since at least the Paleogene and infected a broad range of mammalian species. *Retrovirology*, 16(1), 33. https://doi.org/10.1186/s12977-019-0495-9

Inman, R. M., Magoun, A. J., Persson, J., & Mattisson, J. (2012). The wolverine's niche: Linking reproductive chronology, caching, competition, and climate. *Journal of Mammalogy*, 93(3), 634–644. https://doi.org/10.1644/11-MAMM-A-319.1

Inoue, K., Maeda, N., Mori, T., Sekimoto, R., Tsushima, Y., Matsuda, K., Yamaoka, M., Suganami, T., Nishizawa, H., Ogawa, Y., Funahashi, T., & Shimomura, I. (2014). Possible involvement of Opa-interacting protein 5 in adipose proliferation and obesity. *PLoS One*, 9(2), e87661. https://doi.org/10.1371/journal.pone.0087661

Jeffares, D. C., Jolly, C., Hoti, M., Speed, D., Shaw, L., Rallis, C., Balloux, F., Dessimoz, C., Bähler, J., & Sedlazeck, F. J. (2017). Transient structural variations have strong effects on quantitative traits and reproductive isolation in fission yeast. *Nature Communications*, 8, 14061. https://doi.org/10.1038/ncomms14061

Jewgenow, K., Goeritz, F., Neubauer, K., Fickel, J., & Naidenko, S. V. (2006). Characterization of reproductive activity in captive male Eurasian lynx (*Lynx lynx*). *European Journal of Wildlife Research*, 52(1), 34–38. https://doi.org/10.1007/s10344-005-0002-6

Johnson, R. J., & Andrews, P. (2010). Fructose, uricase, and the back-to-Africa hypothesis. *Evolutionary Anthropology*, 19(6), 250–257. https://doi.org/10.1002/evan.20266

Kalyaanamoorthy, S., Minh, B. Q., Wong, T. K. F., von Haeseler, A., & Jermiin, L. S. (2017). ModelFinder: fast model selection for accurate phylogenetic estimates. *Nature Methods*, 14(6), 587–589. https://doi.org/10.1038/nmeth.4285

Kashtanov, S. N., Svischeva, G. R., Pishchulina, S. L., Lazebny, O. E., Meshchersky, I. G., Simakin, L. V., & Rozhnov, V. V. (2015). Geographical structure of the sable (*Martes zibellina* L.) gene pool on the basis of microsatellite loci analysis. *Russian Journal of Genetics*, 51(1), 69–79.

Kassal, B. Y., & Sidorov, G. N. (2013). Distribution of the sable (*Martes zibellina*) and the pine marten (*Martes martes*) in Omsk Oblast and biogeographic effects of their hybridization. *Russian Journal of Biological Invasions*, 4(2), 105–115. https://doi.org/10.1134/S2075111713020070

Kim, B.-M., Lee, Y. J., Kim, J.-H., Kim, J.-H., Kang, S., Jo, E., Lee, S. J., Lee, J. H., Chi, Y. M., & Park, H. (2020). The genome assembly and annotation of the southern elephant seal *Mirounga leonina*. *Genes*, 11(2), https://doi.org/10.3390/genes11020160

Koepfli, K.-P., Deere, K. A., Slater, G. J., Begg, C., Begg, K., Grassman, L., Lucherini, M., Veron, G., & Wayne, R. K. (2008). Multigene phylogeny of the Mustelidae: Resolving relationships, tempo and biogeographic history of a mammalian adaptive radiation. *BMC Biology*, 6, 10. https://doi.org/10.1186/1741-7007-6-10

Kosiol, C., Vinar, T., da Fonseca, R. R., Hubisz, M. J., Bustamante, C. D., Nielsen, R., & Siepel, A. (2008). Patterns of positive selection in six Mammalian genomes. *PLoS Genetics*, 4(8), e1000144. https://doi.org/10.1371/journal.pgen.1000144

Krebs, J., Lofroth, E., Copeland, J., Banci, V., Cooley, D., Golden, H., Magoun, A., Mulders, R., & Shults, B. (2004). Synthesis of survival rates and causes of mortality in North American wolverines. *Journal of Wildlife Management*, 68(3), 493–502.

Kriventseva, E. V., Kuznetsov, D., Tegenfeldt, F., Manni, M., Dias, R., Simão, F. A., & Zdobnov, E. M. (2019). OrthoDB v10: sampling the diversity of animal, plant, fungal, protist, bacterial and viral genomes

for evolutionary and functional annotations of orthologs. *Nucleic Acids Research*, *47*(D1), D807–D811. https://doi.org/10.1093/nar/gky1053

Kronenberg, Z. N., Osborne, E. J., Cone, K. R., Kennedy, B. J., Domyan, E. T., Shapiro, M. D., Elde, N. C., & Yandell, M. (2015). Wham: Identifying structural variants of biological consequence. *PLoS Computational Biology*, *11*(12), e1004572. https://doi.org/10.1371/journal.pcbi.1004572

Langmead, B., & Salzberg, S. L. (2012). Fast gapped-read alignment with Bowtie2. *Nature Methods*, *9*(4), 357–359. https://doi.org/10.1038/nmeth.1923

Larivière, S., & Ferguson, S. H. (2003). Evolution of induced ovulation in North American Carnivores. *Journal of Mammalogy*, *84*(3), 937–947. https://doi.org/10.1644/BME-003

Law, C. J., Slater, G. J., & Mehta, R. S. (2018). Lineage diversity and size disparity in Musteloidea: Testing patterns of adaptive radiation using molecular and fossil-based methods. *Systematic Biology*, *67*(1), 127–144. https://doi.org/10.1093/sysbio/syx047

Layer, R. M., Chiang, C., Quinlan, A. R., & Hall, I. M. (2014). LUMPY: A probabilistic framework for structural variant discovery. *Genome Biology*, *15*(6), R84. https://doi.org/10.1186/gb-2014-15-6-r84

Lee, J.-E., Oh, H.-A., Song, H., Jun, J. H., Roh, C.-R., Xie, H., Dey, S. K., & Lim, H. J. (2011). Autophagy regulates embryonic survival during delayed implantation. *Endocrinology*, *152*(5), 2067–2075. https://doi.org/10.1210/en.2010-1456

Lennox, A. R., & Goodship, A. E. (2008). Polar bears (*Ursus maritimus*), the most evolutionary advanced hibernators, avoid significant bone loss during hibernation. *Comparative Biochemistry and Physiology. Part A, Molecular & Integrative Physiology*, *149*(2), 203–208. https://doi.org/10.1016/j.cbpa.2007.11.012

Lewin, H. A., Graves, J. A. M., Ryder, O. A., Graphodatsky, A. S., & O'Brien, S. J. (2019). Precision nomenclature for the new genomics. *GigaScience*, *8*(8), https://doi.org/10.1093/gigascience/giz086

Li, B., Wolsan, M., Wu, D., Zhang, W., Xu, Y., & Zeng, Z. (2014). Mitochondrial genomes reveal the pattern and timing of marten (*Martes*), wolverine (*Gulo*), and fisher (*Pekania*) diversification. *Molecular Phylogenetics and Evolution*, *80*, 156–164. https://doi.org/10.1016/j.ympev.2014.08.002

Li, H., & Durbin, R. (2011). Inference of human population history from individual whole-genome sequences. *Nature*, *475*(7357), 493–496.

Lim, H. J., & Song, H. (2014). Evolving tales of autophagy in early reproductive events. *The International Journal of Developmental Biology*, *58*(2–4), 183–187. https://doi.org/10.1387/ijdb.130337hl

Liu, G., Zhao, C., Xu, D., Zhang, H., Monakhov, V., Shang, S., Gao, X., Sha, W., Ma, J., Zhang, W., Tang, X., Li, B., Hua, Y., Cao, X., Liu, Z., & Zhang, H. (2020). First draft genome of the sable, *Martes zibellina*. *Genome Biology and Evolution*, *12*(3), 59–65. https://doi.org/10.1093/gbe/evaa029

Lopes, F. L., Desmarais, J., Gevry, N. Y., Ledoux, S., & Murphy, B. D. (2003). Expression of vascular endothelial growth factor isoforms and receptors Flt-1 and KDR during the peri-implantation period in the mink, *Mustela vison*. *Biology of Reproduction*, *68*(5), 1926–1933.

Löytynoja, A. (2014). Phylogeny-aware alignment with PRANK. *Methods in Molecular Biology*, *1079*, 155–170.

Lynch, M., & Conery, J. S. (2000). The evolutionary fate and consequences of duplicate genes [Review of The evolutionary fate and consequences of duplicate genes]. *Science*, *290*(5494), 1151–1155.

Maglott, D., Ostell, J., Pruitt, K. D., & Tatusova, T. (2011). Entrez Gene: Gene-centered information at NCBI. *Nucleic Acids Research*, *39*(Database issue), D52–D57. https://doi.org/10.1093/nar/gkq1237

Martinez, B., & Ortiz, R. M. (2017). Thyroid hormone regulation and insulin resistance: Insights from animals naturally adapted to fasting. *Physiology*, *32*(2), 141–151. https://doi.org/10.1152/physiol.00018.2016

McGee-Lawrence, M., Buckendahl, P., Carpenter, C., Henriksen, K., Vaughan, M., & Donahue, S. (2015). Suppressed bone remodeling in black bears conserves energy and bone mass during hibernation. *The Journal of Experimental Biology*, *218*(Pt 13), 2067–2074. https://doi.org/10.1242/jeb.120725

McLaren, W., Gil, L., Hunt, S. E., Riat, H. S., Ritchie, G. R. S., Thormann, A., Flicek, P., & Cunningham, F. (2016). The Ensembl variant effect predictor. *Genome Biology*, *17*(1), 122. https://doi.org/10.1186/s13059-016-0974-4

McNutt, J. W., Groom, R., & Woodroffe, R. (2019). Ambient temperature provides an adaptive explanation for seasonal reproduction in a tropical mammal. *Journal of Zoology*, *309*(3), 153–160. https://doi.org/10.1111/jzo.12712

Mead, R. A. (1981). Delayed implantation in mustelids, with special emphasis on the spotted skunk. *Journal of Reproduction and Fertility* *29*, 11–24.

Mead, R. A. (1989). The physiology and evolution of delayed implantation in carnivores. In J. L. Gittleman (Ed.), *Carnivore behavior, ecology, and evolution* (pp. 437–464). Springer US.

Mendes, F. K., & Hahn, M. W. (2016). Gene tree discordance causes apparent substitution rate variation. *Systematic Biology*, *65*(4), 711–721. https://doi.org/10.1093/sysbio/syw018

Mérot, C., Oomen, R. A., Tigano, A., & Wellenreuther, M. (2020). A roadmap for understanding the evolutionary significance of structural genomic variation. *Trends in Ecology & Evolution*, *35*(7), 561–572. https://doi.org/10.1016/j.tree.2020.03.002

Minh, B. Q., Hahn, M. W., & Lanfear, R. (2020). New methods to calculate concordance factors for phylogenomic datasets. *Molecular Biology and Evolution*, *37*(9), 2727–2733. https://doi.org/10.1093/molbev/msaa106

Minh, B. Q., Schmidt, H. A., Chernomor, O., Schrempf, D., Woodhams, M. D., von Haeseler, A., & Lanfear, R. (2020). IQ-TREE 2: New models and efficient methods for phylogenetic inference in the genomic era. *Molecular Biology and Evolution*, *37*(5), 1530–1534. https://doi.org/10.1093/molbev/msaa015

Miranda, I., Giska, I., Farelo, L., Pimenta, J., Zimova, M., Bryk, J., Dalén, L., Mills, L. S., Zub, K., & Melo-Ferreira, J. (2021). Museomics dissects the genetic basis for adaptive seasonal colouration in the least weasel. *Molecular Biology and Evolution*, *38*(10), 4388–4402. https://doi.org/10.1093/molbev/msab177

Mizuarai, S., Miki, S., Araki, H., Takahashi, K., & Kotani, H. (2005). Identification of dicarboxylate carrier Slc25a10 as malate transporter in de novo fatty acid synthesis. *Journal of Biological Chemistry*, *280*(37), 32434–32441. https://doi.org/10.1074/jbc.M503152200

Monakhov, V. G. (2011). Martes zibellina (Carnivora: Mustelidae). *Mammalian Species*, *43*(876), 75–86. https://doi.org/10.1644/876.1

Montaseri, A., Giampietri, C., Rossi, M., Riccioli, A., Del Fattore, A., & Filippini, A. (2020). The role of autophagy in osteoclast differentiation and bone resorption function. *Biomolecules*, *10*(10), https://doi.org/10.3390/biom10101398

Morales-Simfors, N., Bundschuh, J., Herath, I., Inguaggiato, C., Caselli, A. T., Tapia, J., Choquehuayta, F. E. A., Armienta, M. A., Ormachea, M., Joseph, E., & López, D. L. (2020). Arsenic in Latin America: A critical overview on the geochemistry of arsenic originating from geothermal features and volcanic emissions for solving its environmental consequences. *Science of the Total Environment*, *716*, 135564. https://doi.org/10.1016/j.scitotenv.2019.135564

Mustonen, A.-M., Käkelä, R., Käkelä, A., Pyykönen, T., Aho, J., & Nieminen, P. (2007). Lipid metabolism in the adipose tissues of a carnivore, the raccoon dog, during prolonged fasting. *Experimental Biology and Medicine*, *232*(1), 58–69.

Mustonen, A.-M., Puukka, M., Saarela, S., Paakkonen, T., Aho, J., & Nieminen, P. (2006). Adaptations to fasting in a terrestrial mustelid, the sable (*Martes zibellina*). *Comparative Biochemistry and Physiology. Part A, Molecular & Integrative Physiology*, *144*(4), 444–450. https://doi.org/10.1016/j.cbpa.2006.03.008

Nelson, D. W. M., Crossland, M. R., & Shine, R. (2011). Foraging responses of predators to novel toxic prey: effects of predator learning and relative prey abundance. *Oikos*, *120*(1), 152–158. https://doi.org/10.1111/j.1600-0706.2010.18736.x

Nielsen, R., Bustamante, C., Clark, A. G., Glanowski, S., Sackton, T. B., Hubisz, M. J., Fledel-Alon, A., Tanenbaum, D. M., Civello, D., White, T. J., J. Sninsky, J., Adams, M. D., & Cargill, M. (2005). A scan for positively selected genes in the genomes of humans and chimpanzees. *PLoS Biology*, *3*(6), e170. https://doi.org/10.1371/journal.pbio.0030170

Nieminen, P., Käkelä, R., Pyykönen, T., & Mustonen, A.-M. (2006). Selective fatty acid mobilization in the American mink (*Mustela vison*) during food deprivation. *Comparative Biochemistry and Physiology. Part B, Biochemistry & Molecular Biology*, *145*(1), 81–93. https://doi.org/10.1016/j.cbpb.2006.06.007

Nieminen, P., & Mustonen, A.-M. (2007). Uniform fatty acid mobilization from anatomically distinct fat depots in the sable (*Martes zibellina*). *Lipids*, *42*(7), 659–669. https://doi.org/10.1007/s11745-007-3061-5

O'Brien, S. J., Graphodatsky, A. S., & Perelman, P. L. (2020). *Atlas of mammalian chromosomes*. John Wiley & Sons.

Okamoto, T., Imaizumi, K., & Kaneko, M. (2020). The role of tissue-specific ubiquitin ligases, RNF183, RNF186, RNF182 and RNF152, in disease and biological function. *International Journal of Molecular Sciences*, *21*(11), https://doi.org/10.3390/ijms21113921

Olson, M. V. (1999). When less is more: gene loss as an engine of evolutionary change. *American Journal of Human Genetics*, *64*(1), 18–23. https://doi.org/10.1086/302219

Pacifici, M., Santini, L., Di Marco, M., Baisero, D., Francucci, L., Grottolo Marasini, G., Visconti, P., & Rondinini, C. (2013). Generation length for mammals. *Nature Conservation*, *5*, 89–94. https://doi.org/10.3897/natureconservation.5.5734

Papin, C., Rouget, C., Lorca, T., Castro, A., & Mandart, E. (2004). XCdh1 is involved in progesterone-induced oocyte maturation. *Developmental Biology*, *272*(1), 66–75. https://doi.org/10.1016/j.ydbio.2004.04.018

Pasitschniak-Arts, M., & Larivière, S. (1995). Gulo gulo. *Mammalian Species*, *499*, 1–10.

Peng, C., Niu, L., Deng, J., Yu, J., Zhang, X., Zhou, C., Xing, J., & Li, J. (2018). Can-SINE dynamics in the giant panda and three other Caniformia genomes. *Mobile DNA*, *9*, 32. https://doi.org/10.1186/s13100-018-0137-0

Peng, X., Alföldi, J., Gori, K., Eisfeld, A. J., Tyler, S. R., Tisoncik-Go, J., Brawand, D., Law, G. L., Skunca, N., Hatta, M., Gasper, D. J., Kelly, S. M., Chang, J., Thomas, M. J., Johnson, J., Berlin, A. M., Lara, M., Russell, P., Swofford, R., ... Katze, M. G. (2014). The draft genome sequence of the ferret (*Mustela putorius* furo) facilitates study of human respiratory disease. *Nature Biotechnology*, *32*(12), 1250–1255. https://doi.org/10.1038/nbt.3079

Plummer, M., Best, N., Cowles, K., & Vines, K. (2006). CODA: convergence diagnosis and output analysis for MCMC. *R News*, *6*(1), 7–11.

Poglayen-Neuwall, I., Durrant, B. S., Swansen, M. L., Williams, R. C., & Barnes, R. A. (1989). Estrous cycle of the tayra, *Eira barbara*. *Zoo Biology*, *8*(2), 171–177. https://doi.org/10.1002/zoo.1430080208

Poon, C. E., Lecce, L., Day, M. L., & Murphy, C. R. (2014). Mucin 15 is lost but mucin 13 remains in uterine luminal epithelial cells and the blastocyst at the time of implantation in the rat. *Reproduction, Fertility, and Development*, *26*(3), 421–431. https://doi.org/10.1071/RD12313

Poplin, R., Ruano-Rubio, V., DePristo, M. A., Fennell, T. J., Carneiro, M. O., Van der Auwera, G. A., Kling, D. E., Gauthier, L. D., Levy-Moonshine, A., Roazen, D., Shakir, K., Thibault, J., Chandran, S., Whelan, C., Lek, M., Gabriel, S., Daly, M. J., Neale, B., MacArthur, D. G., & Banks, E. (2018). Scaling accurate genetic variant discovery to tens of thousands of samples. *bioRxiv*, 201178. https://doi.org/10.1101/201178

Porubsky, D., Sanders, A. D., Höps, W., Hsieh, P., Sulovari, A., Li, R., Mercuri, L., Sorensen, M., Murali, S. C., Gordon, D., Cantsilieris, S., Pollen, A. A., Ventura, M., Antonacci, F., Marschall, T., Korbel, J. O., & Eichler, E. E. (2020). Recurrent inversion toggling and great ape genome evolution. *Nature Genetics*, *52*(8), 849–858. https://doi.org/10.1038/s41588-020-0646-x

Proulx, G., & Aubry, K. B. (2017). The Martes complex: A monophyletic clade that shares many life-history traits and conservation challenges. In: G. Proulx (Ed.). *The Martes Complex in the 21st Century: ecology and conservation* (pp. 3–24). Mammal Research Institute, Polish Academy of Sciences.

Ranwez, V., Harispe, S., Delsuc, F., & Douzery, E. J. P. (2011). MACSE: Multiple alignment of coding SEquences accounting for frameshifts and stop codons. *PLoS One*, *6*(9), e22594. https://doi.org/10.1371/journal.pone.0022594

Reis, A., Chang, H.-Y., Levasseur, M., & Jones, K. T. (2006). APCcdh1 activity in mouse oocytes prevents entry into the first meiotic division. *Nature Cell Biology*, *8*(5), 539–540. https://doi.org/10.1038/ncb1406

Ren, X., Aleshin, M., Jo, W. J., Dills, R., Kalman, D. A., Vulpe, C. D., Smith, M. T., & Zhang, L. (2011). Involvement of N-6 adenine-specific DNA methyltransferase 1 (N6AMT1) in arsenic biomethylation and its role in arsenic-induced toxicity. *Environmental Health Perspectives*, *119*(6), 771–777.

Reynolds, A., Qiao, H., Yang, Y., Chen, J. K., Jackson, N., Biswas, K., Holloway, J. K., Baudat, F., de Massy, B., Wang, J., Höög, C., Cohen, P. E., & Hunter, N. (2013). RNF212 is a dosage-sensitive regulator of crossing-over during mammalian meiosis. *Nature Genetics*, *45*(3), 269–278. https://doi.org/10.1038/ng.2541

Rinker, D. C., Specian, N. K., Zhao, S., & Gibbons, J. G. (2019). Polar bear evolution is marked by rapid changes in gene copy number in response to dietary shift. *Proceedings of the National Academy of Sciences of the United States of America*, *116*(27), 13446–13451. https://doi.org/10.1073/pnas.1901093116

Sato, J. J., Wolsan, M., Prevosti, F. J., D'Elía, G., Begg, C., Begg, K., Hosoda, T., Campbell, K. L., & Suzuki, H. (2012). Evolutionary and biogeographic history of weasel-like carnivorans (Musteloidea). *Molecular Phylogenetics and Evolution*, *63*(3), 745–757. https://doi.org/10.1016/j.ympev.2012.02.025

Sayyari, E., & Mirarab, S. (2016). Fast coalescent-based computation of local branch support from quartet frequencies. *Molecular Biology and Evolution*, *33*(7), 1654–1668. https://doi.org/10.1093/molbev/msw079

Schweitzer, L. D., Comb, W. C., Bar-Peled, L., & Sabatini, D. M. (2015). Disruption of the rag-ragulator complex by c17orf59 inhibits mTORC1. *Cell Reports*, *12*(9), 1445–1455. https://doi.org/10.1016/j.celrep.2015.07.052

Serão, N. V. L., Veroneze, R., Ribeiro, A. M. F., Verardo, L. L., Braccini Neto, J., Gasparino, E., Campos, C. F., Lopes, P. S., & Guimarães, S. E. F. (2011). Candidate gene expression and intramuscular fat content in pigs. *Journal of Animal Breeding and Genetics*, *128*(1), 28–34. https://doi.org/10.1111/j.1439-0388.2010.00887.x

Shi, G., Xing, L., Liu, Z., Qu, Z., Wu, X., Dong, Z., Wang, X., Gao, X., Huang, M., Yan, J., Yang, L., Liu, Y., Ptácek, L. J., & Xu, Y. (2013). Dual roles of FBXL3 in the mammalian circadian feedback loops are important for period determination and robustness of the clock. *Proceedings of the National Academy of Sciences of the United States of America*, *110*(12), 4750–4755. https://doi.org/10.1073/pnas.1302560110

Shumate, A., & Salzberg, S. L. (2020). *Liftoff: an accurate gene annotation mapping tool*. https://doi.org/10.1101/2020.06.24.169680

Siepka, S. M., Yoo, S.-H., Park, J., Song, W., Kumar, V., Hu, Y., Lee, C., & Takahashi, J. S. (2007). Circadian mutant Overtime reveals F-box

protein FBXL3 regulation of cryptochrome and period gene expression. *Cell*, *129*(5), 1011–1023. https://doi.org/10.1016/j.cell.2007.04.030

Simão, F. A., Waterhouse, R. M., Ioannidis, P., Kriventseva, E. V., & Zdobnov, E. M. (2015). BUSCO: Assessing genome assembly and annotation completeness with single-copy orthologs. *Bioinformatics*, *31*(19), 3210–3212. https://doi.org/10.1093/bioinformatics/btv351

Singh, B. N., Gong, W., Das, S., Theisen, J. W. M., Sierra-Pagan, J. E., Yannopoulos, D., Skie, E., Shah, P., Garry, M. G., & Garry, D. J. (2019). Etv2 transcriptionally regulates Yes1 and promotes cell proliferation during embryogenesis. *Scientific Reports*, *9*(1), 9736. https://doi.org/10.1038/s41598-019-45841-5

Smit, A. F. A. (2004). Repeat-masker open-3.0. http://www.repeatmasker.org and https://ci.nii.ac.jp/naid/10029514778/

Soley, F. G., & Alvarado-Díaz, I. (2011). Prospective thinking in a mustelid? *Eira barbara* (Carnivora) cache unripe fruits to consume them once ripened. *Die Naturwissenschaften*, *98*(8), 693–698. https://doi.org/10.1007/s00114-011-0821-0

Sonna, L. A., Fujita, J., Gaffin, S. L., & Lilly, C. M. (2002). Invited review: Effects of heat and cold stress on mammalian gene expression. *Journal of Applied Physiology*, *92*(4), 1725–1742. https://doi.org/10.1152/japplphysiol.01143.2001

Subramanian, A. R., Kaufmann, M., & Morgenstern, B. (2008). DIALIGN-TX: greedy and progressive approaches for segment-based multiple sequence alignment. *Algorithms for Molecular Biology*, *3*, 6. https://doi.org/10.1186/1748-7188-3-6

Svishcheva, G. R., & Kashtanov, S. N. (2011). Reproductive strategy of the sable (*Martes zibellina* Linnaeus, 1758): An analysis of litter size inheritance in farm-raised populations. *Russian Journal of Genetics: Applied Research*, *1*(3), 221–225. https://doi.org/10.1134/S2079059711030129

Tavori, H., Rashid, S., & Fazio, S. (2015). On the function and homeostasis of PCSK9: Reciprocal interaction with LDLR and additional lipid effects. *Atherosclerosis*, *238*(2), 264–270. https://doi.org/10.1016/j.atherosclerosis.2014.12.017

The UniProt Consortium (2017). UniProt: the universal protein knowledgebase. *Nucleic Acids Research*, *45*(D1), D158–D169.

Thomas, J. H. (2007). Rapid birth-death evolution specific to xenobiotic cytochrome P450 genes in vertebrates. *PLoS Genetics*, *3*(5), e67. https://doi.org/10.1371/journal.pgen.0030067

Tigano, A., Colella, J. P., & MacManes, M. D. (2020). Comparative and population genomics approaches reveal the basis of adaptation to deserts in a small rodent. *Molecular Ecology*, *29*(7), 1300–1314. https://doi.org/10.1111/mec.15401

Totikov, A., Tomarovsky, A., Prokopov, D., Yakupova, A., Bulyonkova, T., Derezanin, L., Rasskazov, D., Wolfsberger, W. W., Koepfli, K.-P., Oleksyk, T. K., & Kliver, S. (2021). Chromosome-level genome assemblies expand capabilities of genomics for conservation biology. *Genes*, *12*(9), 1336. https://doi.org/10.3390/genes12091336

Viscarra, J. A., Rodriguez, R., Vazquez-Medina, J. P., Lee, A., Tift, M. S., Tavoni, S. K., Crocker, D. E., & Ortiz, R. M. (2013). Insulin and GLP-1 infusions demonstrate the onset of adipose-specific insulin resistance in a large fasting mammal: Potential glucogenic role for GLP-1. *Physiological Reports*, *1*(2), e00023. https://doi.org/10.1002/phy2.23

Wang, J., Lu, Z.-X., Tokheim, C. J., Miller, S. E., & Xing, Y. (2015). Species-specific exon loss in human transcriptomes. *Molecular Biology and Evolution*, *32*(2), 481–494. https://doi.org/10.1093/molbev/msu317

Webb, J. K., Brown, G. P., Child, T., Greenlees, M. J., Phillips, B. L., & Shine, R. (2008). A native dasyurid predator (common planigale, Planigale maculata) rapidly learns to avoid a toxic invader. *Austral Ecology*, *33*(7), 821–829.

Weischenfeldt, J., Symmons, O., Spitz, F., & Korbel, J. O. (2013). Phenotypic impact of genomic structural variation: Insights from and for human disease. *Nature Reviews. Genetics*, *14*(2), 125–138. https://doi.org/10.1038/nrg3373

Weisenfeld, N. I., Kumar, V., Shah, P., Church, D. M., & Jaffe, D. B. (2017). Direct determination of diploid genome sequences. *Genome Research*, *27*(5), 757–767. https://doi.org/10.1101/gr.214874.116

Weissensteiner, M. H., Bunikis, I., Catalán, A., Francoijs, K.-J., Knief, U., Heim, W., Peona, V., Pophaly, S. D., Sedlazeck, F. J., Suh, A., Warmuth, V. M., & Wolf, J. B. W. (2020). Discovery and population genomics of structural variation in a songbird genus. *Nature Communications*, *11*(1), 3403. https://doi.org/10.1038/s41467-020-17195-4

Wellenreuther, M., & Bernatchez, L. (2018). Eco-evolutionary genomics of chromosomal inversions. *Trends in Ecology & Evolution*, *33*(6), 427–440. https://doi.org/10.1016/j.tree.2018.04.002

Wilcox, A., Katsanakis, K. D., Bheda, F., & Pillay, T. S. (2004). Asb6, an adipocyte-specific ankyrin and SOCS box protein, interacts with APS to enable recruitment of elongins B and C to the insulin receptor signaling complex. *Journal of Biological Chemistry*, *279*(37), 38881–38888. https://doi.org/10.1074/jbc.M406101200

Wilson, D. E., Mittermeier, R. A. (2009). Family Mustelidae. In: *Handbook of the mammals of the world* (vol. *1*, pp. 627–637). Lynx Editions.

Wu, X., Quondamatteo, F., Lefever, T., Czuchra, A., Meyer, H., Chrostek, A., Paus, R., Langbein, L., & Brakebusch, C. (2006). Cdc42 controls progenitor cell differentiation and beta-catenin turnover in skin. *Genes & Development*, *20*(5), 571–585.

Wu, Z., Latendorf, T., Meyer-Hoffert, U., & Schröder, J.-M. (2011). Identification of trichohyalin-like 1, an s100 fused-type protein selectively expressed in hair follicles. *Journal of Investigative Dermatology*, *131*(8), 1761–1763. https://doi.org/10.1038/jid.2011.71

Xing, Y., & Lee, C. (2006). Alternative splicing and RNA selection pressure–evolutionary consequences for eukaryotic genomes. *Nature Reviews. Genetics*, *7*(7), 499–509. https://doi.org/10.1038/nrg1896

Yang, Z. (2007). PAML 4: Phylogenetic analysis by maximum likelihood. *Molecular Biology and Evolution*, *24*(8), 1586–1591. https://doi.org/10.1093/molbev/msm088

Yu, Y.-H., Chang, Y.-C., Su, T.-H., Nong, J.-Y., Li, C.-C., & Chuang, L.-M. (2013). Prostaglandin reductase-3 negatively modulates adipogenesis through regulation of PPARγ activity. *Journal of Lipid Research*, *54*(9), 2391–2399. https://doi.org/10.1194/jlr.M037556

Zhang, C., Rabiee, M., Sayyari, E., & Mirarab, S. (2018). ASTRAL-III: polynomial time species tree reconstruction from partially resolved gene trees. *BMC Bioinformatics*, *19*(Suppl 6), 153. https://doi.org/10.1186/s12859-018-2129-y

Zhang, H., Ge, Y., He, P., Chen, X., Carina, A., Qiu, Y., Aga, D. S., & Ren, X. (2015). Interactive effects of N6AMT1 and As3MT in arsenic biomethylation. *Toxicological Sciences: An Official Journal of the Society of Toxicology*, *146*(2), 354–362. https://doi.org/10.1093/toxsci/kfv101

Zhang, J. (2003). Evolution by gene duplication: an update. *Trends in Ecology & Evolution*, *18*(6), 292–298. https://doi.org/10.1016/S0169-5347(03)00033-8

Zhang, J., Nielsen, R., & Yang, Z. (2005). Evaluation of an improved branch-site likelihood method for detecting positive selection at the molecular level. *Molecular Biology and Evolution*, *22*(12), 2472–2479. https://doi.org/10.1093/molbev/msi237

Zhang, Z., Li, J., Zhao, X.-Q., Wang, J., Wong, G.-K.-S., & Yu, J. (2006). KaKs_Calculator: Calculating Ka and Ks through model selection and model averaging. *Genomics, Proteomics & Bioinformatics*, *4*(4), 259–263. https://doi.org/10.1016/S1672-0229(07)60007-2

Zhou, Y.-B., Newman, C., Xu, W.-T., Buesching, C. D., Zalewski, A., Kaneko, Y., Macdonald, D. W., & Xie, Z.-Q. (2011). Biogeographical variation in the diet of Holarctic martens (genus Martes, Mammalia: Carnivora: Mustelidae): adaptive foraging in generalists. *Journal of Biogeography*, *38*(1), 137–147. https://doi.org/10.1111/j.1365-2699.2010.02396.x

SUPPORTING INFORMATION

Additional supporting information may be found in the online version of the article at the publisher's website.